infrastructures

MDPI

Article

The 2025 Construction-Stage Collapse of the Jianzha Yellow River Super Bridge: A Document-Based Forensic Engineering Synthesis

Oğuzhan Çetindemir

Construction Equipment Operator Program, Department of Motor Vehicles and Transportation Technologies, Vocational School, İstanbul Okan University, Akfırat, 34959 Tuzla, İstanbul, Türkiye; oguzhan.cetindemir@okan.edu.tr

Abstract

On 22 August 2025, a partially erected section of the Jianzha Yellow River Super Bridge collapsed during cable-tensioning operations, causing 13 fatalities and leaving 3 persons missing. The bridge was being designed as a 366 m main-span continuous steel truss arch, which was erected via cantilever construction supported by a temporary cable-supported fastening system. This document-based forensic engineering synthesis uses the published official investigation report and independently accessed design and technical literature. No independent site inspection, component examination, raw data review, original video review, or validated nonlinear collapse reconstruction was undertaken; the exact instant and progressive development of splice failure are not visible in the report-reproduced chronology and remain unresolved. The official investigation identified bolt-group shear failure and separation at a tower-top distribution beam splice as the initiating physical event following second-stage tensioning of the No. 4 tie cable. These accident-specific findings are not redetermined in the present study; its original contribution is the evidence-status separation and engineering synthesis of the reported evidence through construction-stage load-path reconstruction, connection mechanics assessment, quantitative consistency checks, robustness interpretation, and safety barrier analysis. The reported bolt deficiencies are examined through a limited author-derived normalization combining the material-strength and threaded shear-plane effects at the individual-fastener level; this indicator is used only as a consistency check and is not interpreted as bolt-group or complete splice capacity. Enlarged and irregular holes, missing fasteners, and unauthorized field modifications are interpreted as further impairing bolt-group load sharing. The evidence-constrained load-path assessment indicates that the officially identified splice separation would have interrupted a primary temporary support path while the permanent arch action had not yet developed. Visible cantilever descent was followed by cable rupture, arch-rib fracture, and extensive collapse within approximately 10 s. A qualitative fault-tree and bow-tie analysis organizes the reported procurement, fabrication, design, installation, inspection, monitoring, and governance deficiencies and identifies high-leverage preventive, verification, and consequence-limiting barrier pathways. The findings support consequence-based classification, independent verification, formal hold points, robustness assessment, and personnel exclusion for safety-critical temporary works.

Keywords: bridge collapse; bridge construction; Jianzha Yellow River Bridge; China; mega projects; Xining–Chengdu Railway; lesson learned; under construction; bridge monitoring; construction stage analysis

Check for updates

Academic Editors: Miao Su, Zhiping Zeng, Min Wu and Fuming Wang

Received: 26 July 2026
Revised: 28 August 2026
Accepted: 30 August 2026
Published: 2 September 2026

Copyright: © 2026 by the author. Licensee MDPI, Basel, Switzerland. This article is an open access article distributed under the terms and conditions of the Creative Commons Attribution (CC BY) license.

1. Introduction

Bridge failures occurring during construction differ fundamentally from failures of completed bridges because structural configuration, restraints, boundary conditions, load paths, and redundancy change between erection stages. Construction-stage reliability therefore cannot be inferred solely from the adequacy of the completed bridge and should be evaluated for each safety-critical erection configuration [1–3]. The importance of such stage-specific assessment has also been demonstrated by Zucca et al. [4], who showed through staged numerical analysis that an unplanned re-tensioning operation increased demand at a critical structural node and contributed to the construction-stage collapse mechanism of a post-tensioned reinforced-concrete truss bridge.

This distinction is particularly important for long-span arch and cable-supported bridges. Before arch closure, the permanent load path and global stability system are incomplete, and partially erected ribs and deck segments may depend on temporary towers, tie cables, backstays, anchorage beams, distribution beams, and bracing. During this phase, these nominally temporary components may function as primary load-bearing elements, and their loss can remove a critical force-transfer path supporting substantial portions of the incomplete structure.

Safety requirements for temporary works have consequently evolved toward consequence-based reliability specification [1,5]. Because construction stages generally involve shorter exposure periods than the permanent design situation, the appropriate reliability target need not be identical to that of the completed structure and may be calibrated to both exposure duration and failure consequence [1]. Although permanent structure reliability increasingly incorporates structural system redundancy [6], temporary works reliability remains less unified [7–9], and bridge-failure surveys continue to identify temporary works and erection-stage components as important contributors to construction-stage failures [8,10–12]. Recent research has therefore emphasized stage-specific analysis of cable-supported bridges [13,14], including steel arch and tied-arch systems erected by cantilevering with temporary stays [15–17].

Nevertheless, temporary works may still be treated institutionally as construction means and methods rather than as safety-critical structural systems. Comparative guidance therefore emphasizes defined responsibilities, documented design control procedures, checking proportionate to structural complexity and failure consequence, and controlled authorization throughout the temporary works lifecycle [18]. Gaps between global structural analysis and local-detail verification can leave consequential connections insufficiently assessed. The I-35W deck truss collapse illustrates this broader principle: calculations undertaken for construction loading considered the principal truss members but not the inadequately designed gusset plates that ultimately initiated failure [19]. Although the I-35W accident involved an in-service bridge subjected to concentrated construction loads rather than an incomplete erection system, it demonstrates a broader principle directly relevant to construction-stage safety: the resistance of the global structural system cannot exceed that of its most consequential load-transfer detail.

Connection quality is therefore central to bridge safety. Bolted connection behavior depends on fastener properties, bolt and hole geometry, alignment, thread position relative to the shear plane, plate contact, installation conditions, and fastener engagement. Oversized or irregular holes, missing fasteners, and field modifications may produce differential slip, nonuniform load sharing, and progressive redistribution within the bolt group [20–22]. Where alternative load paths are limited, loss of a single member or connection can produce disproportionate system-level consequences, emphasizing the need for robustness assessment under explicit local-damage or component-removal scenarios [5,6,23–25].

Construction monitoring provides an additional, but not independent, detective barrier. Global quantities such as cable force, cantilever geometry, and tower inclination can identify departures from expected construction-stage response but cannot verify local material conformity, hole geometry, or fastener engagement. Local connection measurements may improve detection of abnormal response, although abrupt internal failure may provide little actionable warning. Monitoring should therefore supplement preventive quality controls, while structural robustness and personnel exclusion remain necessary where intervention time is limited [25–27].

Document-based failure investigation requires traceable separation between observations, source-reported findings, calculations, engineering interpretations, and unresolved uncertainty [28]. Fault-tree, bow-tie, barrier, and organizational accident frameworks additionally provide structured means of relating physical failure to preventive, detective, consequence-limiting, and organizational controls [29–32].

Against this background, the collapse of the Jianzha Yellow River Super Bridge provides an important contemporary case for bridge engineering. The bridge forms part of the Xining–Chengdu Railway in Qinghai Province, China. Its principal crossing was designed as a three-span, double-track continuous steel truss arch with spans of 141 + 366 + 141 m, erected using cantilever construction assisted by a temporary cable-supported system [33,34]. At approximately 03:01 on 22 August 2025, part of the nearly completed main bridge collapsed during the pre-closure construction stage, resulting in 13 fatalities, 3 missing persons, and direct economic losses of approximately CNY 48.86 million [35]. Early reporting attributed the accident to the visible rupture of a construction cable. The official investigation, released on 8 April 2026, concluded that bolt-group shear failure and separation at a tower-top distribution beam splice was the initiating physical event following second-stage tensioning of the No. 4 tie cable. In the load-path interpretation developed here, loss of continuity at that splice would have interrupted a primary temporary support path before arch closure; the exact time and progressive development of the splice failure remain unknown [35].

The official investigation did not attribute the accident to an extraordinary environmental action or to a general lack of capacity in the permanent bridge concept. Instead, it identified an initiating failure in a comparatively localized component of the temporary erection system, followed by system-level collapse [35]. The official investigation further identified deficiencies extending beyond the physical connection, including the procurement of nonconforming bolts, uncontrolled subcontracted fabrication, deficient installation, ineffective inspection and acceptance, inadequate monitoring and supervision, and failures of safety responsibility across the participating organizations [35]. On the basis of the official findings, the case may be interpreted as involving three interacting layers: the defective physical connection, reported failures of technical controls that should have prevented or detected the deficiencies, and reported organizational weaknesses that allowed the temporary component to be fabricated and accepted without adequate verification.

Pre-accident publications describe the intended structural system, erection concept, and principal bridge characteristics [33,34], whereas the official investigation report provides the controlling accident-specific findings, including the chronology, initiating splice failure, material and dimensional deficiencies, construction-stage loading conclusions, and organizational findings [35]. These findings are not redetermined in the present study but constitute the evidentiary basis for the subsequent engineering analysis.

No peer-reviewed English-language study was identified that integrates this accident evidence within a construction-stage load-path, connection mechanics, robustness, and safety barrier framework while explicitly separating official findings from author-derived analysis and interpretation. The individual analytical tools used here—including load-

path tracing, conventional bolted connection mechanics, component removal reasoning, and qualitative barrier analysis—are established methods and are not claimed as novel. The contribution instead lies in their evidence-graded integration to clarify the structural significance of the failed splice, provide bounded quantitative and mechanical consistency checks, distinguish observed chronology from unresolved propagation processes, and identify transferable intervention pathways.

Accordingly, the study distinguishes three levels of output: (1) accident-specific findings reported by the official investigation; (2) author-derived evidence mapping, load-path and topology reconstruction, quantitative consistency checks, connection mechanics interpretation, temporal analysis, robustness assessment, and qualitative barrier analysis; and (3) transferable temporary works lessons concerning consequence-based classification, local-detail verification, field-change control, monitoring, robustness, and personnel exclusion. The study does not independently redetermine the accident cause or reconstruct the complete as-built splice capacity or nonlinear collapse response; the source access limitations are defined in Section 2.

2. Evidence, Methodology, and Limitations

2.1. Research Design and Evidence Status

This study adopted a document-based forensic engineering case study methodology. The official investigation report [35] was treated as the controlling source for accident-specific chronology, physical findings, test results, construction-stage loading conclusions, and organizational findings, while independently accessed design publications, standards, and engineering literature were used for structural context, mechanical interpretation, and transferable recommendations. The author was not affiliated with the investigation team and did not independently access the accident site, recovered components, original footage, raw test or monitoring data, original structural models, or underlying third-party calculations. Independent work was therefore limited to evidence classification, transparent calculations using reported values, load-path and robustness interpretation, barrier analysis, and literature synthesis. These general source access limitations apply throughout the study and are repeated subsequently only where they materially affect a specific interpretation.

To distinguish the contribution of the present study from that of the official investigation, all substantive information was classified into four categories:

1. Official findings: Conclusions explicitly reached by the official investigation team, including the reported initiating component, material test results, dimensional nonconformities, construction-stage loading conclusions, accident chronology, and organizational deficiencies.
2. Evidence reproduced through the official investigation report: Measurements, photographs, video-frame descriptions, material test findings, site observations, and third-party calculation results that were described or reproduced in the report but whose original records were not independently accessed by the author.
3. Author-derived analysis: Transparent calculations or analytical arrangements produced in this study using reported values, including elapsed-time calculations, normalized individual-bolt resistance calculations, evidence-status mapping, construction-stage load-path schematization, and safety barrier classification.
4. Engineering interpretation and literature synthesis: Mechanically supported inferences and recommendations developed by relating the reported evidence to established concepts in bolt-group mechanics, staged construction, structural robustness, monitoring, temporary works reliability, and organizational accident analysis.

These evidence labels are used consistently throughout the manuscript. Author-derived interpretations are not presented as independently verified forensic facts, and

unresolved matters are identified explicitly as uncertainties. Table 1 operationalizes this distinction, while transferable outputs are developed further in Sections 6.5, 7, 7.1–7.4 and 8.

Table 1. Separation between official findings and the contribution of the present study.

Analysis Topic	Official Finding or Report-Reproduced Evidence	Author-Derived Analysis	Additional Engineering Interpretation or Synthesis	Associated Uncertainty
Initiating failure location	Bolt-group shear failure and separation at the tower-top distribution beam splice were identified as the initiating physical failure.	No independent redetermination of the initiating component was performed.	The splice is interpreted as a safety-critical construction-stage load-transfer connection.	Recovered components were not independently inspected; the exact onset and progression of splice failure remain unresolved.
Bolt mechanical properties	The M27 bolts had a 27% deficiency in converted design shear strength and an approximately 20% reduction in effective area due to the threaded shear plane.	The two reported effects are combined into a normalized individual-bolt resistance indicator; see Section 4.3.	The splice is interpreted as a shear/bearing-type bolted connection. The indicator applies only to the individual-fastener resistance term, not to the bolt group, complete splice, or distribution beam assembly.	Raw test data, measured shear plane geometry, preload records, complete bolt-group geometry, plate properties, and the complete splice calculation were unavailable. The sensitivity range is illustrative, not statistical.
Hole geometry and installation	Oversized and irregular holes, a maximum dimension of 32.75 mm, missing bolts, and unauthorized welded modifications were documented.	The maximum hole dimension was 4.75 mm greater than the specified 28 mm, representing an approximate 17% increase.	Variable clearances are interpreted as permitting sequential engagement, nonuniform load sharing, and redistribution within the bolt group.	Complete bolt pattern, individual hole measurements, contact conditions, and fastener-engagement sequence were unavailable.
Construction-stage force quantities	The No. 4 tie-cable pair comprised eight bundles, four per main truss. Reported values were 1112 tf (10.90 MN) design demand, 1200 tf (11.77 MN) monitoring control force, 1884 tf (18.48 MN) nominal distribution beam resistance, and 3120 tf (30.60 MN) nominal cable resistance.	Reported forces were converted to SI units and organized on a common single main truss basis for comparison.	Calculated ratios are nominal design-level comparisons only and do not represent the capacity–demand ratio of the as-built splice.	The single main truss scope of the 1200, 1884, and 3120 tf values is author-interpreted. Original monitoring instructions, tower calculations, raw force histories, and the complete splice model were unavailable.
Post-tensioning interval and visible collapse chronology	Second-stage tensioning was reported complete at approximately 02:56; visible descent began at 03:01:40, followed by cable rupture at 03:01:42, arch-rib fracture at 03:01:45, and extensive collapse at 03:01:50.	A nominal unobserved interval of 5 min 40 s and an approximately 10 s visible collapse phase were calculated.	Delayed connection degradation is mechanically plausible but unverified; the elapsed interval alone does not establish progressive damage or instantaneous overload at 02:56.	The timing of jacking pressure, unloading, lock-off, force transfer, and internal damage remain unresolved; the 02:56 time was reported only to the minute.
Construction-stage load path and transverse topology	The report describes paired upstream/downstream main-truss-side support paths, including tie cables, anchorage beams, distribution beams, tower legs, and backstays, with failure at a distribution beam splice.	Two longitudinal support lines were schematized, and unilateral, bilateral, or rapidly coupled splice loss scenarios were evaluated.	Splice separation is interpreted as interrupting at least the affected support line. Unilateral loss could cause asymmetric/torsional redistribution; bilateral or rapidly coupled loss could remove both lines.	Initial failure side, transverse coupling and stiffness, residual force in the opposite line, and torsional response remain unresolved.
Failure propagation	Cantilever descent, cable rupture, arch-rib fracture near A16, and subsequent arch/deck collapse were reported.	The events were organized into an evidence-constrained component removal sequence.	Because descent preceded cable rupture, the cable failure is interpreted as secondary. Load-path loss, redistribution, geometric change, and insufficient arrest response provide a mechanically consistent propagation framework.	Dynamic amplification, transient cable forces, torsional response, lateral/out-of-plane buckling at A16, and fracture localization cannot be quantified from the available data.
Organizational deficiencies and safety barriers	Deficiencies were reported in procurement, material documentation, fabrication, design checking, installation, inspection, monitoring, supervision, hazard identification, and regulatory control.	The findings were organized into a qualitative fault tree, bow-tie model, and barrier-status matrix.	Splice failure remains the initiating physical event; failed technical/organizational controls are treated as contributing factors, while alternative support and personnel exclusion are consequence-limiting controls.	Organizational findings were not independently investigated. Barrier classifications are author-derived; no probabilities, minimal cut sets, or quantitative effectiveness measures were calculated.
Recommendations	The official investigation included accident-specific corrective recommendations.	The study distinguishes accident-specific drivers from established practice and identifies procedural refinements and auditable implementation/verification controls in Section 8.	Transferable recommendations address safety-critical temporary works, local-detail verification, field deviations and hold points, monitoring, robustness, and personnel exclusion.	Applicability depends on structural type, erection method, contractual organization, governing standards, and project-specific risk.

For orientation, the official investigation identified bolt-group shear failure and separation at a tower-top distribution beam splice following second-stage tensioning of the No. 4 tie cable as the initiating physical event. The failure occurred while the arch remained unclosed and dependent on the temporary cable-supported erection system; visible cantilever descent was subsequently followed by cable rupture, arch-rib fracture, and extensive structural collapse [35].

2.2. Evidence Hierarchy and Source Selection

Table 1 classifies the evidentiary and analytical role of individual claims, whereas Table 2 summarizes source provenance and access. No independently accessed primary accident evidence was available.

Table 2. Source access and evidence hierarchy adopted in the study.

Evidence Category	Materials Included	Role in the Study	Access and Independence Limitation
Category I: Independently accessed primary accident evidence	None	Direct verification of accident-specific observations, measurements, tests, records, or components.	No site access, component examination, original video, raw test data, witness statements, monitoring data, or underlying third-party calculations were independently accessed.
Category II: Directly accessed official investigation report	Published official investigation report [35].	Controlling source for accident-specific chronology, causal conclusions, physical findings, construction-stage loading conclusions, and organizational findings.	The report was accessed directly, but the underlying investigation and examinations were not performed by the author.
Category III: Primary accident evidence reproduced through the official report	Test results, site observations, photographs, video-frame descriptions, recovered component information, hole measurements, project records, and third-party calculations reproduced or summarized in [35].	Evidence-constrained interpretation of the official findings.	Multiple evidence types originate from one documentary source; original files, specimens, calculations, and records were not independently accessed.
Category IV: Secondary project and design literature	Pre-collapse design publications and publicly available project descriptions [33,34].	Intended bridge configuration, erection concept, terminology, and design context.	These sources predate the accident and cannot establish the as-built condition or accident cause.
Category V: Standards and broader engineering literature	Fastener and steel standards; monitoring, robustness, forensic, temporary works, and risk analysis literature.	Mechanical interpretation, comparison, calculations, and recommendations.	Provides contextual and mechanical support but cannot independently verify Jianzha-specific facts.
Category VI: Author-derived analysis and interpretation	Unit conversions, elapsed-time calculations, individual-bolt normalization, dimensional comparison, load-path reconstruction, component removal reasoning, and barrier classification.	Original analytical contribution of the present study	Dependent on the completeness and accuracy of the available documentary evidence.
Category VII: Illustrative historical-comparison sources	Official inquiries, governmental archives, and selected peer-reviewed analyses of six purposively selected bridge failures.	Mechanism-based comparison of construction state, initiating deficiency, load-path interruption, propagation, and relevance to Jianzha.	Purposive, non-systematic, and non-exhaustive; heterogeneous cases are not statistically representative of bridge collapses.

The principal accident-specific source was the 62-page official investigation report issued by the Qinghai Provincial Government Accident Investigation Team [35]. It was treated as the controlling source for chronology, causal conclusions, physical findings, construction-stage loading conclusions, and organizational findings. Material test results, dimensional measurements, photographs, video descriptions, project records, and third-party calculations reproduced in that report were not independently accessed and are therefore treated as report-reproduced evidence rather than independent sources. Two pre-collapse design publications [33,34] were used only to establish the intended bridge configuration, erection concept, and terminology; where they differed from the accident-stage configuration documented by the investigation, the official report took precedence.

Standards and broader technical literature were used only to assess mechanical plausibility and support interpretation, comparison, and recommendations. These sources covered bolted connection behavior and applicable steel provisions [20,22,36–38], temporary works

reliability and governance [1,7–9,18], staged analysis of cable-supported and cantilever-erected bridges [2,3,13–16], structural robustness and monitoring [5,6,23–26], forensic and barrier analysis methodology [28–32], and selected historical bridge failures [19,27,39–45]. They were not used to independently verify Jianzha-specific facts.

2.3. Data Extraction and Evidence Coding

A structured evidence matrix was used only to maintain traceability between the documentary sources and subsequent analysis. Extracted information covered the bridge and erection configuration, critical construction operation, physical and material findings, event chronology, and safety controls. Each item was coded as an official finding, report-reproduced evidence, author-derived analysis, or engineering interpretation according to Section 2.1. These categories are coding domains rather than independent evidence streams or analytical methods. Where a statement contained both reported evidence and author interpretation, the two elements were separated. Chinese technical terminology was translated according to engineering meaning.

2.4. Analytical Questions and Outputs

Each procedure addresses a distinct engineering question and produces a defined author-derived output from the official-report evidence; none creates independent accident evidence.

2.4.1. Construction-Stage Load Path, Topology, and Component Removal Reasoning

This procedure addressed the structural role of the officially identified splice before arch closure and the bounded system consequences compatible with its loss. The load path was traced through the temporary cable-supported system, and unilateral, bilateral, or rapidly coupled splice loss scenarios were considered. The resulting output is a bounded topology interpretation showing that splice loss interrupted at least one primary temporary support line and that the observed propagation is compatible with insufficient residual support or arrest capacity. No quantitative analysis was performed regarding load redistribution, torsional effects, residual capacity, or dynamic collapse.

2.4.2. Event Sequence Reconstruction

This procedure distinguished events directly established by the documentary chronology from unresolved internal processes. Reported timestamps and video-frame descriptions were assessed using temporal precedence and load-path compatibility. The resulting output separates the observed sequence—cantilever descent, cable rupture, arch-rib fracture, and extensive collapse—from the unobserved processes preceding visible movement. The post-tensioning interval is therefore treated only as a temporal bound. Detailed results are presented in Section 4.1.

2.4.3. Normalized Individual-Bolt Resistance Assessment

This procedure assessed the combined individual-fastener effect of the two quantitative bolt deficiencies reported by the official investigation: reduced material strength and reduced resisting area at the threaded shear plane. The resulting normalized individual-bolt resistance indicator and sensitivity range are used only as a consistency check and do not estimate bolt-group resistance, complete splice capacity, or the accident-specific capacity–demand ratio. Details are presented in Section 4.3.

2.4.4. Fault-Tree, Bow-Tie, and Barrier Analysis

This procedure identified where independent controls could have prevented, detected, interrupted, or limited the documented failure pathway. The fault-tree and bow-tie rep-

resentations organize preventive and detective controls before loss of continuity, while consequence-limiting controls are mapped after loss of continuity, with barrier status classified from the documentary record. The output is an evidence-constrained ordering of three intervention pathways: material and fabrication conformity, engineering verification and field-change control, and detection/consequence limitation. No probabilities, minimal cut-sets, or quantitative barrier-effectiveness rankings were calculated.

2.5. Selection of Illustrative Historical Bridge Failures

The historical cases were selected purposefully for mechanism-based comparison rather than through a systematic review protocol. Candidate cases were identified from official inquiry reports, governmental archives, established bridge-failure literature, and reference tracing from those sources. A case was retained when it satisfied at least two of the following criteria: (1) collapse occurred during construction or under a construction-related load state; (2) the incomplete or temporarily supported structure depended on a safety-critical erection component; (3) failure initiated in a localized member, connection, diaphragm, support, or temporary works element; (4) fabrication incompatibility, field intervention, design-checking deficiency, or inadequate inspection contributed to the failure; and (5) local failure propagated into disproportionate structural loss. The cases were selected on the basis of mechanism-level relevance to Jianzha rather than direct structural similarity. The resulting set spans different structural forms, historical periods, and failure-control deficiencies, allowing recurrence of higher-level load-path and control mechanisms to be examined across different bridge systems. These differences are not interpreted as evidence of causal equivalence. Because the selection was purposive rather than systematic, the six cases are not claimed to be the only failures satisfying the stated criteria. They were retained as sufficiently documented principal comparators for mechanism-based comparison with the Jianzha collapse; while other relevant failures are used contextually where their relevance is narrower. The comparison is illustrative and not statistically representative, and it is not intended to validate the Jianzha collapse mechanism through historical analogy.

Accordingly, the comparison can support mechanism-level contextualization and the transferability of selected engineering lessons, but it cannot establish structural equivalence, identical causal pathways, quantitative similarity, or independent validation of the Jianzha collapse mechanism. The comparison evaluates five attributes, consolidated into three analytical categories: construction or loading state; initiating deficiency, triggering demand or operation, and collapse propagation; and bounded relevance to Jianzha. Official inquiry or investigation reports were treated as the controlling sources for accident-specific findings, while peer-reviewed or established technical syntheses were used only to supplement the engineering context. For the Second Narrows Bridge, the 1958 British Columbia Royal Commission report [40] was used as the primary source and the later engineering synthesis [37] as a supplementary source.

2.6. Study Limitations

Consistency was assessed within the official report by comparing its chronology, physical observations, test results, dimensional findings, calculations, and excluded alternatives. Because these evidence types were accessed through the same documentary source, agreement among them is treated as within-report consistency rather than independent triangulation. Independently accessed design publications, standards, and technical literature were used only to assess mechanical plausibility and context, not to verify Jianzha-specific facts.

The study is limited by the absence of complete fabrication and shop drawings, the full bolt-group arrangement, individual-test and hole-measurement datasets, bolt-pretension records, the original temporary works model, raw jacking-pressure and cable-force histories, complete monitoring data, original surveillance footage, and independent examination of recovered components. It therefore does not independently calculate complete splice capacity, reconstruct transient collapse response, or reassess legal responsibility.

The historical comparison is additionally limited by purposive case selection and differences in structural system, construction state, historical period, regulatory context, and source accessibility. It identifies bounded mechanism-level analogies and is not intended to establish structural or causal equivalence among the selected failures or independently validate the specific Jianzha collapse mechanism.

3. Bridge and Erection-Stage Load Path

3.1. Bridge and Permanent Structural System

The Jianzha Yellow River Super Bridge is located at the boundary between Jianzha County in Huangnan Tibetan Autonomous Prefecture and Hualong Hui Autonomous County in Haidong City, Qinghai Province, China. It forms part of the Xining–Chengdu Railway and was designated as a controlling structure within construction contract section XCTJ11. The bridge crosses the Yellow River using a long-span continuous steel truss arch intended to carry double-track railway traffic [33–35].

The complete bridge has a reported total length of 1596.2 m. Its principal crossing comprises a three-span continuous steel truss arch with a span arrangement of 141 + 366 + 141 m and a main bridge length of 648 m. The main bridge contains 50 structural panels, has an approximate width of 15 m, and has a reported structural weight of approximately 17,200 t. The arch crown is approximately 130 m above the river surface. Figure 1 shows the bridge elevation, principal span arrangement, and panel/node numbering used to describe the accident-stage structural components.

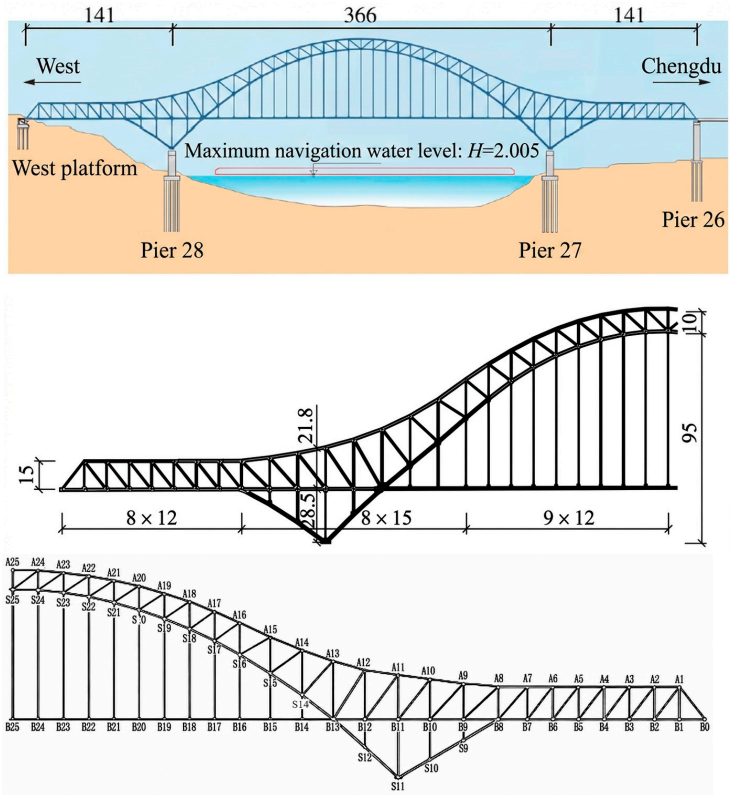


Figure 1. Bridge elevation and panel/node numbering (dimensions are in meters).

In the completed configuration, the bridge was intended to develop an integrated load path through the closed arch, truss and deck system, piers, and foundations. At the accident stage, the arch had not been closed, and the incomplete main-span structure remained dependent on the temporary cable-supported system. The principal parameters of the permanent bridge and temporary erection system are summarized in Table 3.

Table 3. Principal bridge and temporary erection system parameters.

Parameter	Reported Value
Total bridge length	1596.2 m
Main bridge span arrangement	141 + 366 + 141 m
Main bridge length	648 m
Number of main bridge panels	50
Approximate bridge width	15 m
Approximate structural weight	17,200 t
Approximate arch-crown height above water	130 m
Temporary tower height	98 m
Transverse spacing between tower legs	14 m
Tie cable arrangement after modification	Four pairs
Backstay arrangement after modification	Three pairs
Strands per cable bundle	25–30
Nominal strand diameter	15.24 mm
No. 4 monitoring control force	1200 tf, approximately 11.77 MN

Note: Values were obtained from the official investigation report [35]. Force values originally reported in tonne-force were converted using 1 tf = 9.80665 kN. The single main-truss side scope assigned to this value is an author-derived interpretation; see Section 4.4.

3.2. Accident-Stage Erection Configuration

The original erection concept used an arch-first sequence with three tie-cable pairs, three backstay pairs, and vertically separated tower-top anchorage levels. Following reported difficulties in obtaining suitable transport vessels, the scheme was revised to permit simultaneous erection of the arch and deck using deck-based transportation. The revised arrangement used four tie-cable pairs, retained three backstay pairs, and placed the corresponding tower-top anchorages at the same elevation [35].

The official report states that the revision reduced the calculated maximum tie-cable force from 1177 to 1112 tf per main truss and the maximum backstay force from 1283 to 1161 tf per main truss. Comparable completed bridges had used both arch-first and simultaneous erection and both separated and same-level anchorage arrangements. The official investigation did not identify the revised method as the direct cause of collapse; Figure 2 therefore compares the original and revised erection schemes only to define the accident-stage configuration.

3.3. Temporary Load Path and Transverse Topology

The temporary system comprised paired upstream and downstream main-truss-side force-transfer lines. For each line, the incomplete arch and deck transferred force through the lower anchorage beam, four tie-cable bundles, the upper anchorage beam, the associated tower-top distribution-beam line and splice, the corresponding tower leg, the backstays, completed side span, and foundations [35].

The use of plural “distribution beams” in the official account, together with the separate tower legs above the two main trusses, is consistent with paired upstream and downstream tower-top force-transfer lines. However, the complete fabrication drawings and transverse tower-top details were unavailable. It therefore cannot be determined conclusively whether the two distribution beam lines were structurally independent, connected through transverse framing, or capable of substantial force transfer between them.

The official investigation identified failure at a tower-top distribution beam splice, but the publicly available evidence does not resolve whether one main-truss-side splice failed first, whether both sides lost continuity nearly simultaneously, or whether failure of one side rapidly destabilized the other through transverse coupling.

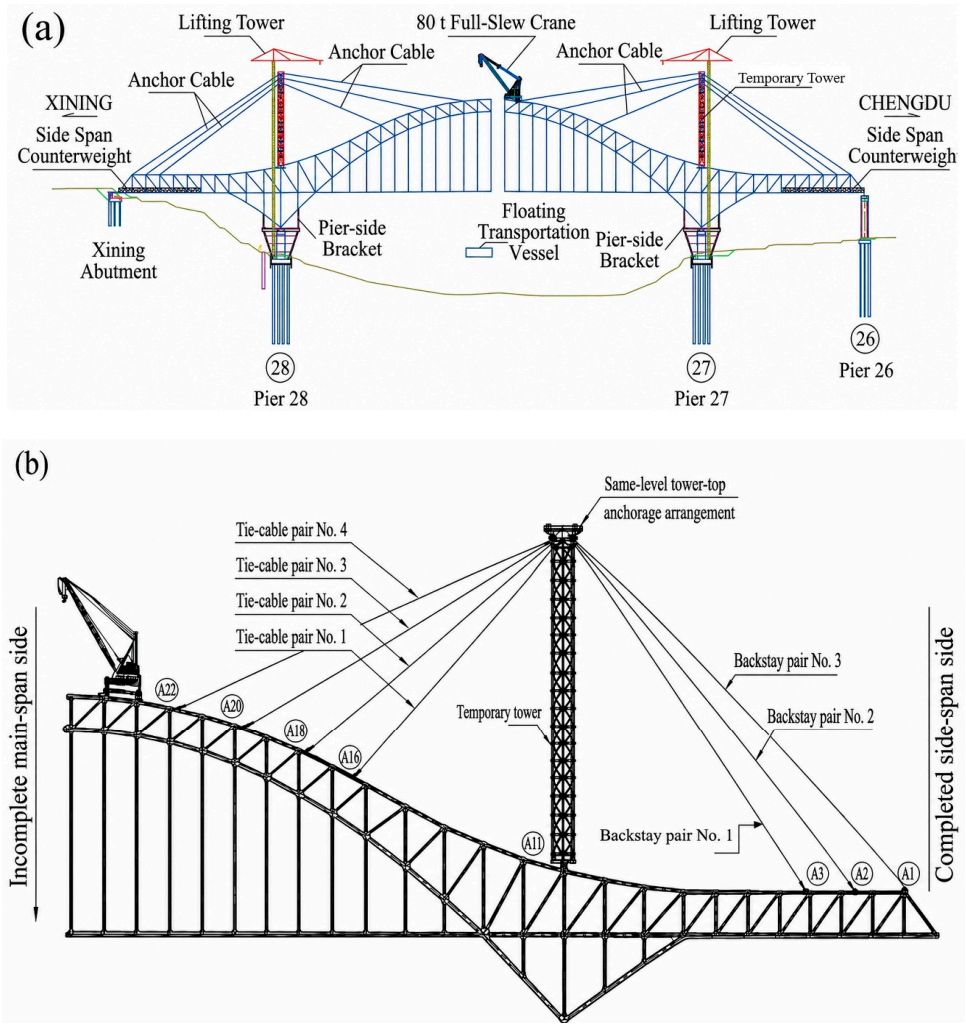


Figure 2. Original and revised erection schemes. (**a**) Original arch-first concept with three tie-cable pairs, three backstay pairs, and vertically separated tower-top anchorage levels. (**b**) Revised accident-stage erection scheme showing four tie-cable pairs, three backstay pairs, and the same-level tower-top anchorage arrangement. The temporary tower was positioned at node A11. The configuration was reconstructed from the official investigation report [35] and is shown to define the accident-stage structural arrangement, not to identify the erection method revision as an independently established cause of collapse.

Two bounded post-failure scenarios are consequently retained. Under a unilateral loss scenario, one main-truss-side support line would initially lose stiffness or continuity while the opposite line could temporarily retain part of its cable force. Such differential support could produce asymmetric cantilever displacement, transverse force redistribution, and torsional demand in the arch, deck, and connecting bracing. Under a bilateral- or rapidly coupled loss scenario, continuity of both main-truss-side support lines would be lost within a short interval. The available force histories, displacement records, transverse stiffness properties, and side-specific damage observations are insufficient to select between these scenarios.

The generally intact condition of the tower legs, cables, anchorage beams, anchorages, and wedges does not establish that those components continued to provide the pre-failure

support force. An intact component can transmit useful force only if a continuous and sufficiently stiff path remains between the cantilever anchorage and the tower and backstay system. The reported sequence shows that global descent was not arrested before secondary failures developed; it does not establish whether a residual path existed briefly, how much force it retained, or when any remaining capacity became insufficient. Figure 3 schematizes the accident-stage erection configuration, the longitudinal force-transfer path of a single main truss side, the paired upstream and downstream tower-top topology, and the bounded unilateral, bilateral, or rapidly coupled splice loss scenarios.

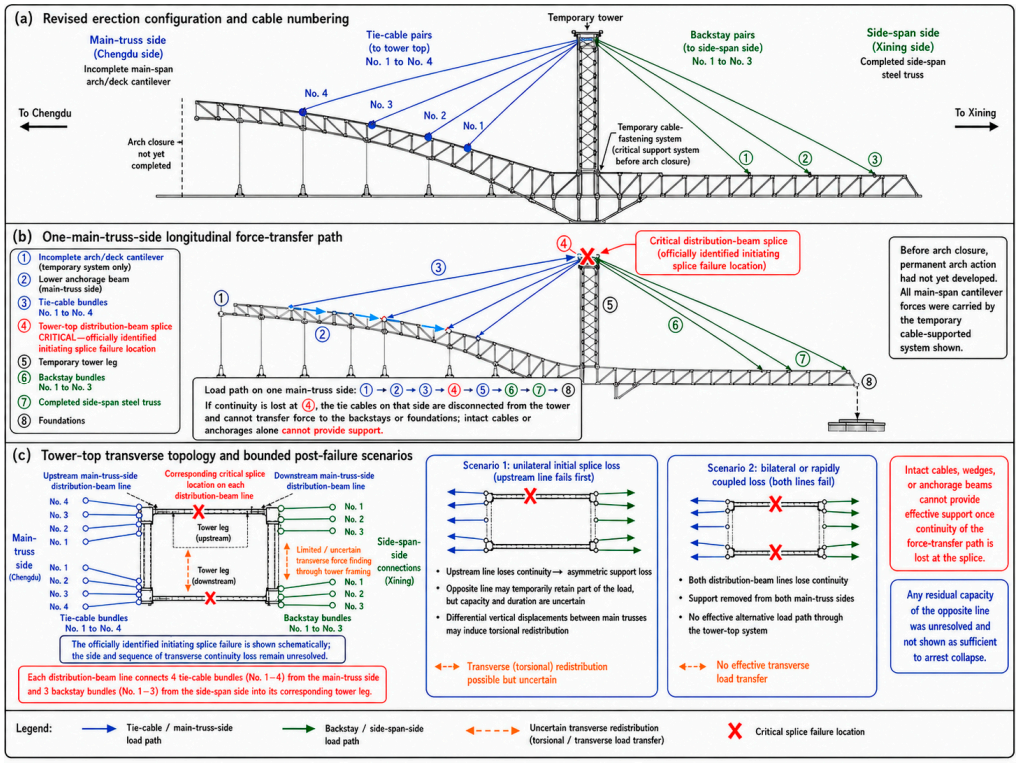


Figure 3. Construction-stage load path, tower-top topology, and bounded splice loss scenarios. (**a**) Revised erection configuration and cable numbering, showing four tie-cable pairs on the incomplete main-span side and three backstay pairs on the completed side-span system. (**b**) Author-derived longitudinal force-transfer path on a single main truss side, tracing the load from the incomplete arch and deck cantilever through the lower anchorage beam, tie-cable bundles, tower-top distribution beam splice, corresponding tower leg, backstays, completed side-span truss, and foundations. The arrows denote the schematic force-transfer path and do not represent the sign of axial force in individual truss members. The red cross identifies the splice location reported by the official investigation as the initiating physical failure. (**c**) Author-derived transverse topology showing paired upstream and downstream main-truss-side distribution beam lines and two bounded post-failure cases: unilateral initial splice loss and bilateral/rapidly coupled loss. Dashed orange arrows denote possible but unquantified transverse or torsional redistribution. The public record does not establish which side lost continuity first, the degree of transverse coupling, or the residual force retained by the opposite line. Accident-stage configuration and component relationships were reconstructed from the official investigation report [35]; force-path, topology, and post-failure scenario interpretations are author-derived.

3.4. Critical Tensioning State

The No. 4 tie-cable pair comprised eight strand bundles, divided as four bundles for each main truss, which were tensioned simultaneously using eight calibrated jacks. Control relied principally on jacking-pressure records and cantilever-tip geometry; direct in situ force measurement of every bundle was not undertaken. The first tensioning stage reached

the reported 67% control level on 21 August 2025. The second stage commenced at 23:39 and was reported complete at approximately 02:56 on 22 August, when the residual upstream and downstream elevation differences at node A25 were 53 and 29 mm, respectively [35].

The publicly available records do not establish whether the reported completion time corresponded to cessation of pumping, continued pressure holding, jack unloading, anchorage lock-off, or complete force transfer. At this stage, the cantilever halves remained unconnected and equilibrium still depended on the temporary cable-supported load path. The associated force quantities and their scope are defined in Section 4.4.

4. Accident Evidence and Connection Assessment

Except where explicitly identified as author-derived analysis or engineering interpretation, the chronology, physical findings, material test results, dimensional observations, reported force quantities, and initiating component discussed in this section are reproduced from the official investigation report [35]. Claim-specific limitations are stated where they materially affect interpretation.

4.1. Visible Chronology and Excluded Alternatives

The chronology reproduced in the official investigation report is summarized in Table 4 and visualized in Figure 4a, while Figure 4b presents the corresponding evidence-constrained component removal and progressive collapse sequence. Second-stage tensioning was reported complete at approximately 02:56, while the first visible cantilever descent occurred at 03:01:40. The No. 1 tie cable ruptured approximately 2 s after descent began, the arch rib fractured near A16 after approximately 5 s, and extensive collapse developed within approximately 10 s [35]. The visible cable rupture is therefore interpreted as secondary to the already developing collapse and not as the initiating event.

Table 4. Reported post-tensioning interval and visible collapse chronology.

Time	Time Relative to First Visible Movement	Observed Event	Engineering Significance
Approximately 02:56	Nominally −5 min 40 s	Second-stage No. 4 tensioning was reported complete, followed by an instruction to terminate tensioning after the geometric check.	Start of the unobserved post-tensioning interval. Jacking pressure, unloading, lock-off, force transfer, connection slip, and internal bolt-group damage remain unresolved.
03:01:40	0 s	The Xining-side main span cantilever began to descend.	First visible evidence of loss of temporary equilibrium.
03:01:42	+2 s	A bright flash propagated along the No. 1 tie cable toward its lower anchorage; the cable ruptured and fell.	Cable rupture occurred after visible descent and is therefore interpreted as secondary to the developing collapse.
03:01:45	+5 s	The arch rib fractured near A16; panels A17–A25 began to fall.	Visible arch-rib fracture and structural propagation developed near A16.
03:01:50	+10 s	Arch panels A17–A25 entered the river; deck panels E15–E25 folded and their leading portion fell.	System-level collapse of the supported arch and deck segments was completed.

Note: Event times and descriptions are reproduced from the official investigation report [35]; the nominal 5 min 40 s interval and relative times after 03:01:40 are author-calculated. Because the reported completion time is only minute-resolved, the pre-movement interval is approximate. The engineering significance column is author-derived and does not establish when internal splice slip or bolt failure began. Original surveillance footage and detailed operational records were not independently accessed.

The nominal interval between reported completion and first visible movement was approximately 5 min 40 s. Because the completion time was reported only to the minute and the relevant operational and deformation records were unavailable, this interval is treated only as a temporal bound; it does not establish when splice damage began, when continuity was fully lost, or whether progressive degradation occurred throughout the interval. Further mechanical interpretation is provided in Section 4.5.

Figure 4 separates the report-reproduced visible chronology from the author-derived bounded component-removal scenarios.

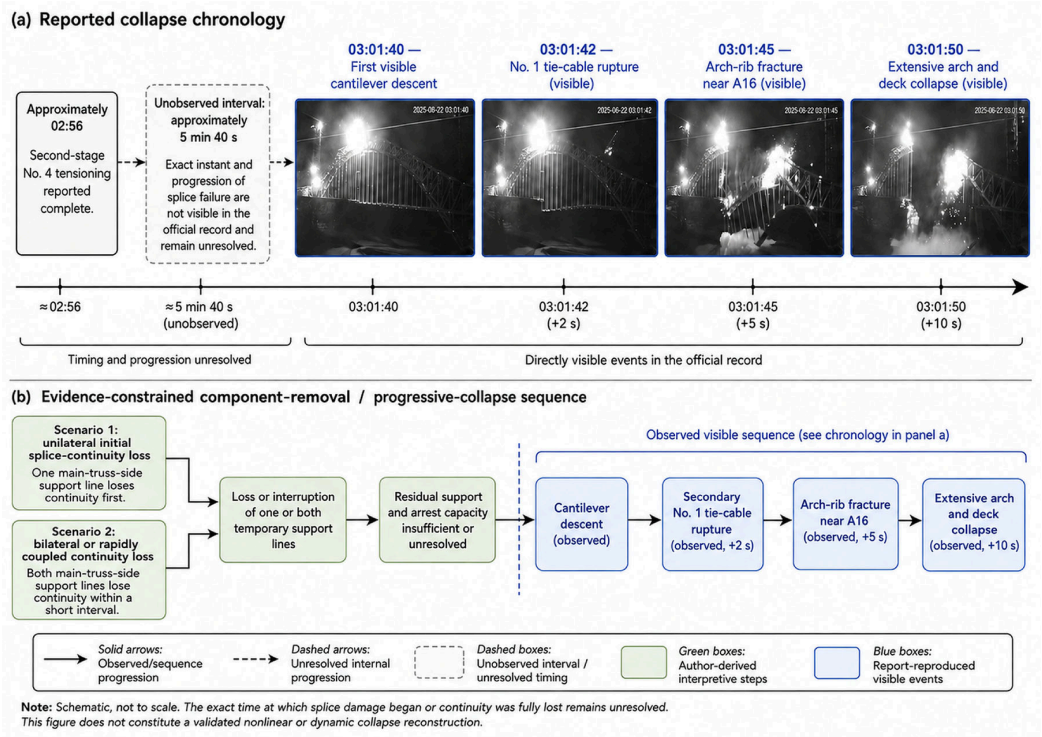


Figure 4. Reported collapse chronology and evidence-constrained component removal and progressive collapse sequence. (**a**) Second-stage No. 4 tensioning was reported complete at approximately 02:56; after an unobserved interval of approximately 5 min 40 s, visible cantilever descent at 03:01:40 was followed by No. 1 tie cable rupture (+2 s), arch-rib fracture near A16 (+5 s), and extensive collapse (+10 s). Surveillance frames are reproduced from ref. [35]. (**b**) Author-derived bounding scenarios for unilateral, bilateral, or rapidly coupled splice continuity loss converging on the reported visible sequence. Exact failure timing, initial side, transverse coupling, and residual force remain unresolved; the schematic is not a validated nonlinear or dynamic reconstruction.

The official investigation excluded earthquake, adverse weather, hydrological effects, inadequate lighting, cable over-tensioning, and initiating failure of the temporary tower, principal cables, anchorage beams, anchorages, or wedges [35]. The collapse is therefore treated as a reported resistance-deficiency failure during an authorized construction operation rather than as a response to an extraordinary external action.

4.2. Initiating Component and Documented Splice Deficiencies

The official investigation identified bolt-group shear failure and separation at the tower-top distribution beam splice as the initiating physical event [35]. The documented deficiencies comprised nonconforming bolt properties and dimensions, threads crossing the shear planes, enlarged and irregular holes, missing fasteners, and unauthorized welded modifications. Table 5 distinguishes the intended connection condition, the documented as-installed condition, and the author's mechanical interpretation.

Table 5. Documented deficiencies in the distribution beam splice.

Parameter or Condition	Intended or Reference Condition	Documented Condition	Mechanical Implication
Bolt designation	Property class 8.8, M27	M27 × 140 and M27 × 180 bolts did not meet the applicable standard	Lower and more variable fastener resistance
Ultimate tensile strength	Compliant property class value	Mean 608.3 MPa; range 583–630 MPa	Reduced tensile and derived shear resistance
Converted design shear strength	Applicable standard requirement	234.5 MPa, reported as 27% below the requirement	Reduced shear resistance
Position of threads	Unthreaded shank intended at the shear plane	Threads entered the splice-plate shear plane	Approximately 20% reduction in effective area resisting shear
Specified hole diameter	28 mm	Most holes larger than specified; maximum measured dimension 32.75 mm	Increased clearance, slip, and nonuniform engagement
Hole shape	Regular and aligned	Oval and hourglass-shaped field-enlarged holes	Altered bolt-group load sharing
Bolt installation	All specified bolts installed	Some bolts omitted	Reduced number of active fasteners
Connection detailing	Bolted splice as designed	Small steel plates welded locally in place of specified bolting	Unverified and nonconforming force-transfer path

The official investigation evaluated the splice through bolt-group shear resistance and explicitly treated the location of the threads at the splice-plate shear plane as a resistance-reducing deficiency [35]. On this evidentiary basis, the present study treats the connection as a shear/bearing-type bolted splice for mechanical interpretation, rather than as a slip-resistant friction joint. The publicly available record does not provide the original bolt-preload records or a slip-resistance design calculation; therefore, the actual installation preload cannot be independently established. The distribution beam splice used M27 × 140 and M27 × 180 bolts specified or marked as property class 8.8. According to the material test results reproduced in the official investigation report, the recovered samples did not satisfy the requirements of GB/T 3098.1-2010 with respect to external dimensions, chemical composition, Vickers and Rockwell hardness, tensile strength, and shear strength [35,44]. The report-reproduced test results also exhibited substantial scatter, indicating inconsistent manufacturing quality rather than a uniform, predictable reduction in one property alone.

The ultimate tensile strengths reproduced in the official investigation report ranged from 583 to 630 MPa, with a mean value of 608.3 MPa. The corresponding converted design shear strength was reported as 234.5 MPa, approximately 27% below the applicable standard requirement. These values indicate that the installed fasteners could not provide the mechanical resistance assumed for compliant property class 8.8 bolts [35].

A second deficiency concerned the length of the threaded portion. The threads extended into the splice-plate shear plane, whereas the design resistance had been based on the larger gross cross-sectional area of the unthreaded bolt shank. The investigation estimated that the effective area resisting shear was thereby reduced by approximately 20% [35].

The investigation found that the flange plates, web plates, and splice plates had not been drilled in accordance with the design. Most holes exceeded the specified 28 mm diameter, substantial misalignment was addressed through field enlargement, and oval and hourglass-shaped openings were documented. The maximum measured hole dimension was 32.75 mm, which was 4.75 mm greater than the specified diameter, representing an approximate 17% increase [35,41,45].

For the mechanical interpretation in this table, the splice is treated as a shear/bearing-type bolted connection on the basis of the bolt-group shear-resistance treatment reported in the official investigation [35]. The intended and documented connection conditions are reproduced from the official investigation report [35]. Unless otherwise stated, the mechanical implication column presents the author's interpretation based on established connection mechanics. The gross M27 shank area of 572.6 mm^2 was calculated from the

nominal bolt diameter, while the threaded area of approximately 459.4 mm^2 is a nominal standard value. The report-implied effective area of approximately 458.1 mm^2 was obtained by applying the reported 20% reduction in the gross shank area; it is not a measured shear-plane area. The normalized remaining resistance estimate and sensitivity range are author-derived and apply only to the reported material strength deficiency and threaded shear-plane area. They do not represent the resistance or failure capacity of the complete splice. The sensitivity range is illustrative and is not a statistical confidence interval.

Figure 5 schematically relates the tower-top force-transfer arrangement to the reported distribution beam splice and documented connection deficiencies. Because complete fabrication drawings and the full as-built bolt-group geometry were unavailable, panels (b) and (c) are explanatory reconstructions only. In Figure 5b, the flange- and web-splice fasteners represent separate bolt groups shown in a common longitudinal projection; their apparent alignment does not imply physical intersection. The enlarged local detail illustrates only the reported thread/shear plane condition of a representative bolt and does not reconstruct the as-built plate stack, number of shear planes, or relative plate thicknesses.

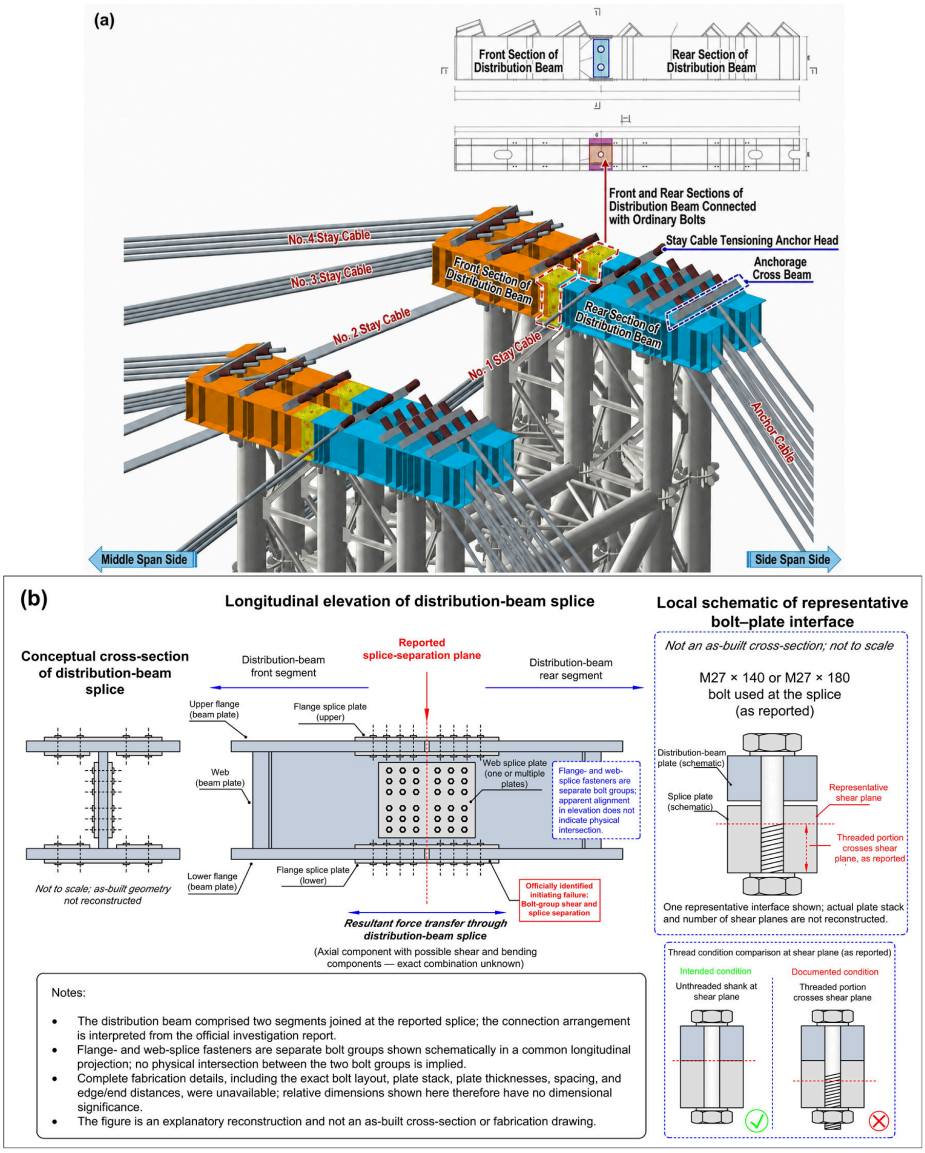


Figure 5. *Cont.*

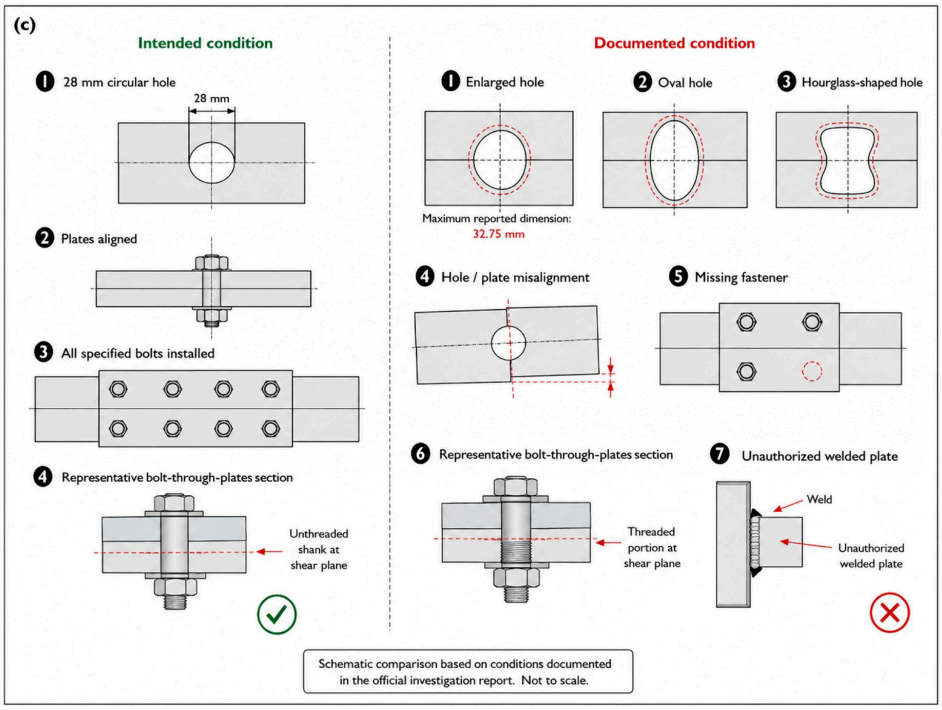


Figure 5. Tower-top distribution beam arrangement and documented splice deficiencies. (**a**) Tower-top configuration showing the distribution beam sections, cable anchorages, and bolted splice. (**b**) Conceptual schematic distinguishing the flange- and web-splice bolt groups; the exact as-built connection geometry is not reconstructed. The local detail shows the documented condition of a representative M27 bolt with the threaded portion crossing the shear plane. (**c**) Intended and documented connection conditions, including enlarged/irregular holes, misalignment, missing fasteners, and unauthorized welded modifications. Panel (**a**) was adapted from the official investigation report [35]; panels (**b**,**c**) are author-derived explanatory schematics and are not to scale.

Variable hole clearance is mechanically significant because bolts in a bearing-type group engage only after local gaps between the bolt shanks and hole boundaries are closed. Differences in hole size, shape, and alignment can therefore cause sequential engagement, localized bearing, and nonuniform force sharing, while connector load-deformation behavior governs the extent of redistribution within the bolt group [20–22]. Reynolds et al. [20] reported average predicted strength reductions of approximately 9%, 14%, and 19% for the oversized-hole categories examined in their analytical study. These values cannot be transferred directly to the Jianzha splice, but they support the general interpretation that enlarged clearances can reduce bolt-group resistance. Because the Jianzha holes were irregular and varied between locations, simultaneous and uniform bolt engagement could not be assumed.

Missing bolts directly reduced the number of active fasteners and changed the stiffness and force distribution of the bolt group. The improvised welded plates could not be treated as verified strengthening because their geometry, weld properties, and force-transfer function were not incorporated into an approved revised design. The combined condition therefore differed materially from the connection idealized in the temporary works calculation.

4.3. Scope and Normalized Individual-Bolt Resistance Assessment

The purpose of this calculation is not to introduce a new bolted connection design method or to reconstruct the resistance of the failed splice. It provides a transparent bolt-level consistency check by combining, on the same normalized resistance term, the two quantitative deficiencies reported by the official investigation: reduced material strength

and reduced resisting area where the threaded portion crossed the shear plane. Its relevance to the collapse interpretation is therefore limited but specific: it quantifies the combined degradation relative to the nominal individual-fastener assumption, while the accident-specific failure of the bolt group and splice remains an official investigation finding rather than an independently reproduced capacity calculation.

For the limited bolt-level comparison, the individual-bolt shear resistance term is expressed in a generalized form consistent with the applicable steel design provisions [41,45]:

$$V_{b,R} = n_v A_v f_{v,b} \tag{1}$$

where $V_{b,R}$ is the individual-bolt shear resistance, n_v is the number of shear planes, A_v is the resisting area at the shear plane, and $f_{v,b}$ is the design shear strength of the bolt material. For the normalized comparison, n_v and all other common resistance factors cancel, so the remaining resistance ratio depends on the ratio of material strength and resisting area.

For the design condition in which the unthreaded M27 shank intersects the shear plane, the gross shank area is calculated as follows:

$$A_g = \frac{\pi d^2}{4} \tag{2}$$

$$A_g = \frac{\pi (27)^2}{4} = 572.6 \text{ mm}^2 \tag{3}$$

For a standard M27 coarse thread, the nominal threaded stress area is approximately 459 mm^2 [44]. This may also be calculated from:

$$A_s = \frac{\pi}{4} (d - 0.9382p)^2 \tag{4}$$

where $d = 27$ mm and the coarse-thread pitch $p = 3$ mm, giving A_s = 459.4 mm^2. The resulting nominal area ratio is expressed as follows:

$$\frac{A_s}{A_g} = \frac{459.4}{572.6} = 0.802 \tag{5}$$

The official investigation described the threaded shear plane as producing an approximately 20% reduction in effective area [35]. Applied to the gross shank area, this corresponds to a report-implied effective area of:

$$A_{eff,report} = 0.80 A_g = 0.80(572.6) = 458.1 \text{ mm}^2 \tag{6}$$

This value is effectively consistent with the nominal M27 threaded stress area. However, it should not be described as a measured area because the report-reproduced information did not include measured thread-root diameters or individual shear-plane area measurements.

The reported converted design shear strength was 234.5 MPa, approximately 27% below the applicable reference value [35]. The normalized remaining strength ratio is therefore:

$$r_f = 1 - 0.27 = 0.73 \tag{7}$$

Because the shear resistance term in Equation (1) is proportional to the product $A_v f_{v,b}$, the two reported reductions are combined multiplicatively:

$$r_V = r_f \, r_A \tag{8}$$

The multiplication does not assume statistical independence between the two deficiencies. It follows algebraically from the product of material strength and resisting area, provided that both reported reductions apply to the same individual-bolt shear resistance term and that the other resistance factors remain unchanged.

Using the rounded ratios reported by the investigation:

$$r_V = 0.73 \times 0.80 = 0.584 \tag{9}$$

The corresponding estimated individual-bolt shear resistance reduction is expressed as follows:

$$\Delta_V = 1 - r_V = 1 - 0.584 = 0.416 \approx 41.6\% \tag{10}$$

Using the nominal M27 area ratio of 459/572.6 rather than the rounded value of 0.80 gives a remaining resistance ratio of approximately 0.585, representing a reduction of approximately 41.5%. The calculation should therefore be interpreted as a central estimate of approximately 41–42% for the two quantified individual-bolt effects. This percentage is a normalized bolt-level resistance effect only and must not be interpreted as a reduction factor for the bolt group, complete splice, or distribution beam assembly.

The report-reproduced ultimate tensile strengths ranged from 583 to 630 MPa, with a mean of 608.3 MPa. If the converted shear strength is assumed to vary in direct proportion to the reported tensile strength range while the nominal area ratio is held constant, the estimated individual-bolt resistance reduction ranges from approximately 39.4% to 43.9%. This is an illustrative sensitivity range rather than a statistical confidence interval because the raw test dataset, specimen-level converted shear strengths, and measured shear-plane areas were unavailable.

The calculation does not quantify the resistance of the complete splice. Complete splice resistance additionally depends on the number and arrangement of installed bolts, the number of shear planes, bolt-group eccentricity, plate bearing, net-section and block-shear resistance, bolt pretension, friction and contact conditions, hole clearances and shapes, connection slip, missing fasteners, sequential bolt engagement, prying or secondary bending, and the resistance of the splice plates and connected beam segments. The information required to evaluate these limit states was not publicly available. For the same reason, an accident-specific shear demand for an individual bolt cannot be determined from the available evidence. The reported demands are available only at the force-path level for a single main truss side; distributing them among individual bolts would require the complete as-built bolt pattern and force-sharing state, which are unavailable. Accordingly, the normalized result is used in this study only as a bolt-level consistency check and is not used to infer bolt-group resistance, splice failure load, or the capacity–demand ratio of the as-built connection.

4.4. Capacity–Demand Context

Table 6 defines the structural scope and analytical role of the reported force quantities. These quantities provide the available demand context at the structural force-path level rather than at the individual-bolt level. The official report explicitly identifies 1112 tf as the revised maximum tie-cable force per main truss. Because the 1200, 1884, and 3120 tf quantities were compared with that value, the present study treats them as applying to one four-bundle main-truss-side force path; this remains an author-derived scope interpretation because the original monitoring instruction and calculations were unavailable.

Table 6. Force scope and normalized capacity–demand framework for the critical No. 4 tensioning stage.

Quantity or Analytical Role	Force Path and Structural Scope	Reported or Derived Value	Normalized Comparison and Limit-State Meaning	Source, Evidence Status, and Uncertainty
Design demand, D_d	Revised maximum tie-cable force for a single main truss; four No. 4 bundles transferring force to the associated tower-top distribution assembly	1112 tf (10.90 MN)	$D_d/D_c = 0.927$; $D_d/R_{db,\mathrm{nom}} = 0.590$. Design-stage demand, not measured accident force.	Explicitly reported per main truss in ref. [35]. Original construction-stage model unavailable.
Monitoring control force, D_c	Prescribed tensioning control target for one No. 4 main-truss-side cable set	1200 tf (11.77 MN)	Reference demand ratio : $D_c/D_c = 1.000$; $D_c/R_{db,\mathrm{nom}} = 0.637$; $D_c/R_{c,\mathrm{nom}} = 0.385$.	Reproduced from monitoring instruction JZHHQ-57 through ref. [35]. It is a control target, not a direct force measurement. The single main truss scope is author-interpreted.
First-stage intended or inferred force, D_1	Procedure-derived force level after the first tensioning stage for the same cable set	Approximately 804 tf (7.89 MN)	$D_1/D_c = 0.670$. Intended or inferred at operational level only.	Calculated from the reported 67% stage in ref. [35]. No direct cable force monitoring was undertaken.
Final accident-stage force, D_f	Force in the same cable set following completion of second-stage tensioning	No direct measurement; official conclusion : $D_f \leq 1200$tf (≤ 11.77 MN)	$D_f/D_c \leq 1.000$; nominally $D_f/R_{db,\mathrm{nom}} \leq 0.637$.	Official investigation conclusion based on jacking records, geometry, and third-party simulation [35]. Raw data and original simulation unavailable.
Nominal distribution-beam resistance, $R_{db,\mathrm{nom}}$	As-designed tower-top distribution beam assembly resisting No. 4 tension for one main-truss-side force path	1884 tf (18.48 MN)	$R_{db,\mathrm{nom}}/D_c = 1.570$. Nominal design resistance only; not as-built splice resistance.	Reported in ref. [35]. Original calculation and precise component decomposition unavailable; the single main truss scope is author-interpreted.
Nominal No. 4 cable resistance, $R_{c,\mathrm{nom}}$	Nominal resistance of the four-bundle No. 4 cable set assigned to one main truss	3120 tf (30.60 MN)	$R_{c,\mathrm{nom}}/D_c = 2.600$ Cable resistance, not distribution beam or splice resistance.	Reported in ref. [35]. Original cable resistance calculation unavailable; the single main truss scope is author-interpreted.
Author- derived individual-bolt resistance ratio, r_V	Individual-bolt shear term considering only reported strength and threaded area effects	Central estimate: 0.585 retained; sensitivity range: 0.561–0.606	Dimensionless bolt-level result. It cannot be applied directly to the 1884 tf distribution beam resistance.	Author-derived in Section 4.3 using report-reproduced inputs. Not a complete splice estimate.
As-built splice resistance and reported governing limit state, $R_{\mathrm{splice,as\text{-}built}}$	Complete splice including bolt-group geometry, holes, missing bolts, plates, contact, eccentricity, and all applicable limit states	Not calculable from available information	The ratio $\frac{D_f}{R_{\mathrm{splice,as\text{-}built}}}$ cannot be calculated independently. Reported governing limit state: bolt-group shear and splice separation.	Official investigation concluded that applied demand exceeded realized resistance [35]. No independent complete splice calculation was possible.

Note: Force values were converted using 1 tf = 9.80665 kN; normalized ratios are author-derived. The single main truss scope assigned to the 1200, 1884, and 3120 tf values is interpreted from the report's four-bundle-per-main-truss arrangement and is not independently verified. The individual-bolt resistance ratio is a bolt-level consistency check and must not be applied to the 1884 tf nominal distribution beam resistance. Individual-bolt demand and as-built splice resistance cannot be determined because the complete bolt-group geometry and force-sharing state are unavailable.

Using the common single main-truss side scope adopted in Table 6, the revised design demand of 1112 tf corresponds to approximately 0.590 of the reported nominal distribution beam resistance (1112/1884) and 0.356 of the nominal No. 4 cable resistance (1112/3120). The 1200 tf monitoring control force corresponds to approximately 0.637 and 0.385 of these respective nominal resistances. Equivalently, the reported nominal distribution beam resistance was approximately 1.69 times the revised design demand and 1.57 times the monitoring control force, while the nominal cable resistance was approximately 2.81 and 2.60 times these respective demand levels. These ratios are nominal design-level comparisons only and do not represent the capacity–demand ratio of the as-built splice.

The numerical comparisons above show that both the revised design demand and the monitoring control force remained below the reported nominal distribution beam and cable resistances. They therefore support the distinction between the nominal design adequacy of the reported force-transfer system and the realized resistance of the defective as-built splice. They do not establish the adequacy of the as-installed connection or independently reproduce its failure capacity. Its complete resistance cannot be calculated from the available bolt-group geometry, plate, contact, and installation information. The conclusion that accident-stage demand exceeded realized splice resistance therefore remains attributable to the official investigation [35].

4.5. Interpretation of the Unobserved Post-Tensioning Interval

The official investigation concluded that the defective splice failed following the authorized second-stage No. 4 tensioning operation [35], but the available chronology does not establish when splice damage began or continuity was fully lost. The nominal 5 min 40 s interval is therefore treated only as an unobserved temporal bound and does not demonstrate progressive damage throughout that period. Given the documented hole clearances, irregular geometry, and bolt deficiencies, connection slip, sequential fastener engagement, localized bearing, nonuniform force sharing, and redistribution remain mechanically plausible [20–22], but their occurrence, timing, and sequence cannot be established from the available evidence.

5. Failure Propagation and Robustness

This section interprets the reported collapse sequence through construction-stage load paths and component removal reasoning. It does not constitute a validated equilibrium, nonlinear, or dynamic reconstruction. The structural interpretation is nevertheless constrained by three quantitative observations available from the public record: (1) the nominal capacity–demand ratios summarized in Table 6; (2) the normalized individual-bolt resistance assessment in Section 4.3; and (3) the measured temporal ordering of the visible collapse events in Table 4 and Figure 4. These quantities are used as consistency checks on the proposed load-path interpretation rather than as inputs to a reconstructed global collapse model.

5.1. Load-Path Interruption and Transverse Uncertainty

The official investigation identified bolt-group shear failure and separation at the tower-top distribution beam splice as the initiating physical event and concluded that the accident-stage demand exceeded the realized resistance of the defective bolt group [35]. In the pre-closure configuration, each main truss side was supported through a longitudinal sequence comprising tie-cable bundles, an upper anchorage beam, a tower-top distribution beam line and splice, and the associated tower leg. The backstays balanced the resulting tower action through the completed side-span system. In the author-derived load-path interpretation, loss of continuity at the officially identified splice would have interrupted

at least one primary construction-stage support line while the gravity loads acting on the incomplete bridge remained.

The publicly available evidence does not establish whether the opposite main-truss-side line retained partial support temporarily, whether both splice lines lost continuity nearly simultaneously, or whether unilateral loss rapidly propagated through transverse coupling. Accordingly, the manuscript does not claim that one splice failure instantaneously removed every cable force. The narrower evidence-supported conclusion is that the visible descent was not arrested before subsequent failures developed; whether a residual path existed briefly, how much force it retained, and when any remaining support became insufficient remain unresolved.

The bounded splice loss scenarios can therefore be stated quantitatively only in topological, rather than force distribution, terms. Before continuity loss, two main-truss-side longitudinal support lines are represented in the accident-stage topology. Under the unilateral bounding case, continuity is lost in one of these two lines while the status and residual force of the opposite line remain unresolved. Under the bilateral- or rapidly coupled bounding case, continuity is lost in both lines. These states should not be interpreted as 50% and 100% reductions in structural resistance or cable force because the force carried by each line and the transverse redistribution between them cannot be reconstructed from the available evidence.

5.2. Visible Propagation

The report-reproduced chronology records the first visible cantilever descent at 03:01:40, followed by rupture of the No. 1 tie cable approximately 2 s later, arch-rib fracture near A16 at approximately +5 s, and extensive collapse by approximately +10 s [35]. Because structural movement preceded cable rupture, the cable failure is interpreted as secondary rather than initiating. These times constrain the visible propagation sequence but do not permit the associated transient member forces or dynamic amplification to be quantified.

The available records do not permit a quantitative explanation of why fracture localized near A16. Member force histories, sectional and connection properties at A16, lateral restraint and bracing characteristics, initial geometric imperfections, fracture-surface evidence, local deformation measurements, and the displacement–time history were unavailable. Although lateral or out-of-plane buckling was not identified as a mechanism in the official investigation, the compressive role that an upper arch member may experience during the evolving construction-stage collapse means that such instability could plausibly have amplified local bending and deformation near A16 after the initial loss of support. Axial force redistribution, bending, lateral or local instability, connection deformation, and impact are therefore retained as possible secondary contributors rather than assigned quantified causal roles.

If splice continuity was initially lost on only one main truss side, the resulting difference in vertical restraint could have generated differential cantilever displacement, transverse force redistribution, and torsional or warping demand in the arch, deck, and connecting bracing. Such a response is mechanically plausible but is not established as a causal contributor because the side-specific release sequence, transverse stiffness, torsional coupling, cable force histories, and displacement–time records are unavailable. A bilateral- or rapidly coupled loss remains equally unresolved. No quantitative magnitude or causal weight is therefore assigned to torsional response.

5.3. Component Removal and Robustness Interpretation

The qualitative component-removal assessment asks whether the incomplete bridge could continue carrying its construction-stage actions after the loss of splice continuity. The two bounded initiation cases and their convergence into the report-reproduced visible collapse sequence are summarized in Figure 4b. The documented sequence is mechanically consistent with interruption of at least one primary main-truss-side support line, insufficient residual support or arrest response, cantilever descent, secondary cable and arch-rib failures, and disproportionate collapse. This assessment establishes pathway consistency only; it does not calculate residual capacity, member demand, collapse time, or dynamic amplification. Component-removal analysis is an established scenario-based approach for examining structural robustness after localized damage, but its conclusions depend on the assumed removal scenario, structural continuity, dynamic effects, and available residual load paths [5,6,23–25].

Taken together, the quantitative checks constrain—but do not uniquely reconstruct—the collapse mechanism. The revised design demand and monitoring control force were approximately 59.0% and 63.7%, respectively, of the reported nominal distribution beam resistance, indicating that the authorized loading level was below the reported nominal resistance of the as-designed assembly. Independently, the bolt-level normalization confirms that the two quantified fastener deficiencies act cumulatively to reduce the individual-bolt shear resistance term relative to its nominal reference; this result is used only as a consistency check and cannot be extended to complete splice resistance. Finally, the observed chronology establishes that global movement preceded cable rupture by approximately 2 s and that major structural propagation occurred within approximately 10 s. These three quantitative observations are mutually consistent with the official finding that a deficient splice lost continuity under an authorized construction-stage loading condition and with the subsequent load-path interpretation developed here. They do not determine whether continuity loss was initially unilateral or bilateral, quantify the residual force in the opposite support line, or reproduce the nonlinear collapse response.

Together, these checks support only a bounded robustness inference: the officially identified splice separation is mechanically consistent with the interruption of at least one main-truss-side temporary support line, while the residual support state, the initial mode of continuity loss (unilateral, bilateral, or rapidly coupled), and the nonlinear collapse response remain unresolved.

The official chronology and reported damage observations were used to assess whether the documented sequence was mechanically consistent with the loss of the distribution beam splice and subsequent collapse propagation; the assessment was not intended to reproduce the exact nonlinear response. The available data were screened for simplified quantitative analysis, but the public record did not provide the accident-stage cable inclinations, panel-by-panel self-weight and erection loads, member sectional properties and joint stiffnesses, transverse coupling characteristics, time history or symmetry of support loss, or displacement–time data. Consequently, the quantitative assessment was limited to evidence-supported capacity–demand ratios, individual-bolt normalization, event timing, and load-path topology. Analyses of accident-specific equilibrium, cantilever bending demand, A16 fracture demand and lateral stability/buckling, dynamic amplification, asymmetric support loss, and nonlinear staged-construction response were not attempted because they would require assumptions for critical quantities unavailable in the public record. Numerical results based principally on such assumed values would create false precision rather than accident-specific evidence.

6. Safety Barrier and Organizational Analysis

6.1. Analytical Framework

The organizational and quality control findings in this section are reproduced or paraphrased from the official investigation report [35]. Their classification as causal, contributing, or consequence-limiting factors and their arrangement within the fault-tree and bow-tie framework are author-derived, using the qualitative risk and barrier concepts described in IEC 31010 and established bow-tie and barrier literature [29,30,32]. Organizational accident theory was used only to interpret how multiple technical and managerial controls may align or fail across organizational levels [31]. The analysis does not independently assign legal or institutional responsibility.

Bolt-group shear failure and separation at the distribution beam splice remain the officially identified physical initiating event. Procurement, fabrication, design, installation, inspection, monitoring, supervision, and governance deficiencies are classified as contributing controls because they enabled the defective splice to enter or remain in service. Alternative support capacity and personnel exclusion are classified separately as consequence-limiting controls. Figure 6 presents the qualitative fault-tree and bow-tie model, while Table 7 provides the corresponding barrier status, evidence basis, and analytical role.

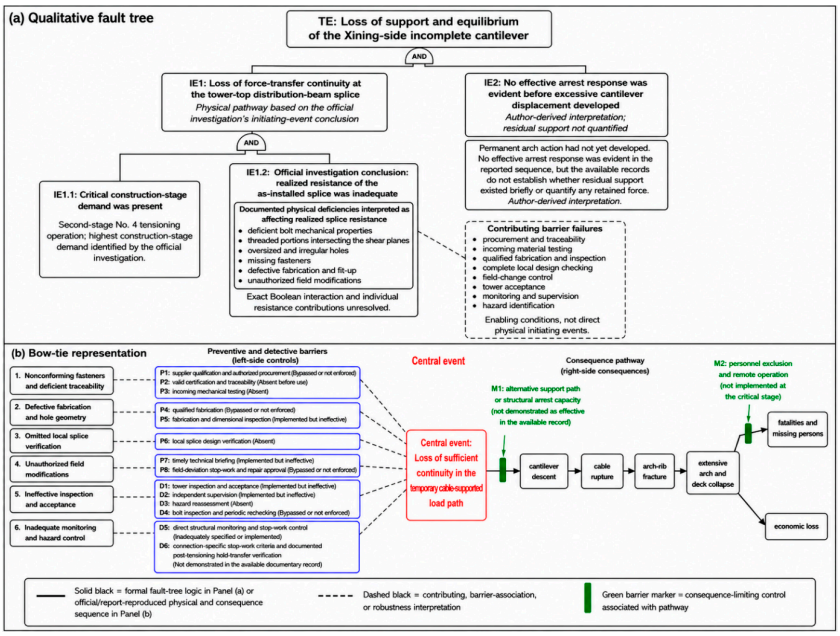


Figure 6. Qualitative accident pathway analysis: (**a**) fault-tree representation of loss of support and equilibrium of the Xining-side incomplete cantilever and (**b**) bow-tie representation of the threats, failed controls, central event, consequences, and consequence-limiting barriers associated with loss of the temporary cable-supported load path. Accident-specific physical and organizational findings are reproduced from the official investigation [35]. Their organization, barrier classification, and logical arrangement are author-derived. Solid black connections in Panel (**a**) represent formal fault-tree logic, while solid black connections in Panel (**b**) represent the documented physical or consequence sequence. Dashed black connections represent contributing barrier association or robustness interpretations for which exact Boolean dependence cannot be established from the available evidence. Green barrier markers identify consequence-limiting controls associated with the relevant consequence pathways. No failure probabilities or quantitative importance measures were calculated. The principal high-leverage barrier pathways interpreted from this arrangement are discussed in Section 6.5; these are qualitative intervention pathways rather than probability-based importance rankings or minimal cut sets.

Table 7. Matrix of barrier functions, documentary status, evidence, and analytical roles.

Barrier or Control	Function	Documentary Status	Evidence Supporting Classification	Analytical Role and Evidence Status
P1. Supplier qualification and authorized procurement	Preventive	Bypassed or not enforced	Supplier was contacted privately before procurement was subsequently completed through the approved platform.	Contributing factor; classification based on official findings in [35].
P2. Valid product certification and material traceability	Preventive	Absent before use	Bolts arrived without required quality documentation; a false certificate was produced after the accident.	Contributing factor; official finding [35].
P3. Incoming mechanical property testing of bolts and steel plates	Preventive	Absent	Bolts and distribution beam plates were used without required incoming testing.	Contributing factor; official finding [35].
P4. Qualified fabrication organization	Preventive	Bypassed or not enforced	Fabrication was assigned to a subcontractor lacking required qualifications, specialist drilling equipment, and demonstrated competence.	Contributing factor; official finding [35].
P5. Fabrication process, dimensional, and weld inspection	Preventive	Implemented but ineffective	Nonconforming hole positions/geometry and fabrication defects were not prevented or detected before use.	Contributing factor; official finding [35].
P6. Complete local design verification of the distribution beam splice	Preventive	Absent	The temporary works calculation omitted a specific resistance check of the distribution beam splice plates.	Contributing factor; official finding [35].
P7. Timely technical briefing and communication of connection criticality	Preventive	Implemented but ineffective	Relevant technical briefings were delivered after installation had begun, limiting their preventive value.	Contributing factor; official finding [35].
P8. Stop work and formal engineering reassessment for field deviations	Preventive	Bypassed or not enforced	Hole enlargement, bolt omission/removal, and welded modifications proceeded without a documented stop work and approved reassessment.	Contributing factor; official finding [35].
D1. Tower self-inspection and formal acceptance	Detective and preventive	Implemented but ineffective	Required inspection/acceptance sequence was reversed, and records described the connection as compliant despite documented deviations.	Contributing factor; official finding [35].
D2. Independent supervision verification	Detective	Implemented but ineffective	Supervision did not identify the omitted splice check or deficiencies in qualification, materials, fabrication, and installation.	Contributing factor; official finding [35].
D3. Hazard identification and risk reassessment following the erection modification	Preventive and detective	Absent	The connection was not recognized as a governing major hazard; no dedicated reassessment followed the erection method change.	Contributing factor; official finding [35].
D4. Bolt inspection, retightening, and periodic rechecking before tensioning	Detective and operational	Bypassed or not enforced	Required inspection, retightening, and periodic rechecking of tower connection bolts were not effectively implemented.	Contributing factor; official finding [35].
D5. Direct monitoring of cable force, temporary member stress, and local splices	Detective	Inadequately specified or implemented	Monitoring emphasized global geometry and omitted local splice response; it could not identify latent bolt material or hole engagement defects.	Contributing factor; official finding [35] and author-derived barrier classification.
D6. Connection-specific stop-work criteria and documented post-tensioning hold-and-transfer verification	Detective and operational	Not demonstrated in the available documentary record	Records of raw jacking pressure, lock-off, splice movement, and second-resolved completion were unavailable.	Unresolved contributing control; author-derived classification based on the documentary limitation.
M1. Alternative support path or structural arrest capacity	Consequence-limiting	Not demonstrated as effective in the available record	Permanent arch action had not developed; splice failure was followed by rapid descent and collapse, while any residual support path or retained force remains unquantified.	Consequence-limiting factor; author-derived load-path and robustness interpretation based on [35].
M2. Personnel exclusion and remote operation during and after critical tensioning	Consequence-limiting	Not implemented at the critical stage	Fifteen tensioning workers and the responsible site technician remained on the structure; 13 persons died and three remained missing.	Consequence-limiting factor; official personnel and consequence findings [35], with author-derived barrier classification.

Note: The initiating physical event remains the bolt-group shear failure and separation of the tower-top distribution beam splice identified by the official investigation [35]. "Contributing factor" denotes a failed control that enabled the defective splice to enter service or remain undetected; it does not denote a separate initiating cause. "Consequence-limiting factor" denotes a control that could have reduced structural propagation or personnel exposure after load-path loss. Accident-specific evidence is reproduced or paraphrased from [35], whereas barrier functions, documentary status, and analytical roles are author-derived classifications and not independent factual or legal determinations. No probabilities, reliability indices, minimal cut sets, or quantitative barrier-effectiveness rankings were calculated.

6.2. Preventive Control Failures

The official investigation reported deficiencies in supplier qualification, procurement authorization, material documentation, incoming testing, subcontractor competence, fabrication control, design checking, technical communication, and field-change management [35]. The bolts reportedly entered service without the required traceable quality documentation and incoming mechanical testing, while fabrication was assigned to an organization lacking the required qualifications and specialist capability. Nonconforming hole positions, dimensions, and weld conditions were not identified before use.

The temporary works calculation did not include a specific resistance check of the distribution beam splice plates. Relevant technical briefings were delivered only after tower installation had progressed, reducing their preventive value. When fit-up problems occurred, hole enlargement, bolt omission, packing plates, and welded modifications were used without documented stop-work, reassessment, and approved repair procedures. In the barrier analysis, these findings correspond to failures or bypassing of controls P1–P8 in Table 7.

6.3. Inspection, Monitoring, and Operational Controls

The official investigation reported that the prescribed self-inspection and final acceptance sequence was not followed effectively and that the acceptance process did not identify the material, fabrication, installation, or design-checking deficiencies [35]. Independent supervision likewise did not detect the omitted splice verification, nonconforming materials, fabrication defects, or unauthorized field changes. These findings are represented by controls D1 and D2 in Table 7.

Construction monitoring emphasized cantilever geometry and did not independently measure all relevant cable forces or local splice response. Global geometry could verify the overall construction state but could not establish bolt material conformity, hole geometry, or uniform fastener engagement. Local strain, splice opening or slip, and connection-zone measurements could have improved detection of abnormal response but could not guarantee warning before abrupt internal bolt-group failure. Effective intervention therefore depended on pre-established alert, action, and stop-work criteria operating before loss of the temporary load path. The approximately 10 s visible collapse phase did not provide a credible interval for manual diagnosis or evacuation after global movement began.

6.4. Responsibility, Hazard Identification, and Oversight

The official investigation described fragmented responsibility among design, procurement, commercial, materials, safety, supervision, and project management functions [35]. Written procedures did not consistently produce effective implementation, and responsibility for verification of safety-critical temporary works was not integrated across participating organizations. The report also stated that the distribution beam connection was not identified as a governing major hazard and that no dedicated risk reassessment followed the erection method modification.

The reported inspection activity focused substantially on general and visible site conditions while the critical temporary works risks remained unidentified. The investigation also described limitations in regional regulatory capacity. These observations are treated as contextual and contributing findings rather than as independent proof that any individual organizational condition alone caused the physical failure.

6.5. Barrier Synthesis and High-Leverage Failure Pathways

Table 7 consolidates the preventive, detective, operational, and consequence-limiting controls, their documentary status, supporting evidence, and analytical role. Preventive

failures allowed the nonconforming splice to be fabricated and installed, while ineffective inspection and monitoring allowed it to remain undetected. In the author-derived consequence analysis, the absence of an arrest response evident in the reported sequence, together with the absence of personnel exclusion, increased the structural and human consequences after continuity was lost. Barrier classifications are author-derived interpretations of the official findings, and no probabilities or quantitative effectiveness measures were calculated. The preventive, detective, operational, and consequence-limiting terminology follows established barrier function concepts [29,30], whereas the status assigned to each Jianzha control remains an author-derived classification of the findings reported in [35].

Within this qualitative framework, the fault-tree and bow-tie analysis identifies three particularly important barrier pathways. The first is a pathway involving material and fabrication conformity, in which deficiencies in supplier qualification, material traceability, incoming mechanical testing, fabrication qualification, and dimensional inspection (P1–P5) allowed nonconforming fasteners and fabrication deficiencies to reach the assembled temporary system. Within this pathway, incoming mechanical property testing (P3) and fabrication/dimensional inspection (P5) represent particularly direct opportunities to detect the documented material and fit-up deficiencies before installation.

The second is a pathway involving engineering verification and field changes. The omitted local verification of the distribution beam splice (P6), ineffective communication of connection criticality (P7), and the bypassed stop-work and engineering-reassessment control for field deviations (P8) allowed a safety-critical connection to be used despite unresolved design and fit-up issues. Formal acceptance and independent supervision (D1–D2), hazard reassessment following the erection modification (D3), and pre-tension bolt inspection and rechecking (D4) constituted additional opportunities to interrupt this pathway before the critical tensioning stage. From an engineering control perspective, P6 and P8 are therefore interpreted as high-leverage preventive barriers, while D1–D4 represent successive verification opportunities after upstream controls had failed.

The third pathway concerns detection and consequence limitation after the defective connection entered service. Local monitoring and connection-specific stop-work criteria (D5–D6) could potentially have improved recognition of abnormal response, but the available evidence does not demonstrate that monitoring could have detected the latent material and fit-up deficiencies before abrupt connection failure. Monitoring should therefore be regarded as supplementary to material verification, local design checking, fabrication control, and formal acceptance rather than as their substitute. After the loss of splice continuity, alternative support or arrest capacity (M1) and personnel exclusion/remote operation (M2) become the principal consequence-limiting barriers. M1 concerns structural propagation, whereas M2 would not prevent the physical failure but directly addresses personnel exposure.

These pathways do not constitute statistically ranked cut sets. The new analytical output of the fault-tree and bow-tie synthesis is not a new accident fact or a reclassification of reported causes but an evidence-constrained ordering of where the failure pathway could have been interrupted. Material testing and fabrication inspection (P3 and P5) represent upstream opportunities before installation; local design verification, field-change control, acceptance, supervision, hazard reassessment, and pre-tension inspection (P6–P8 and D1–D4) provide successive opportunities before critical loading; local monitoring and stop-work criteria (D5–D6) act only as supplementary downstream detection; and alternative support or arrest capacity and personnel exclusion (M1–M2) limit consequences after continuity is lost. This ordering distinguishes prevention, verification, detection, and mitigation and shows why downstream monitoring cannot substitute for upstream material, fabrication, and design controls. It provides the analytical basis for prioritiz-

ing the procedural recommendations in Section 8 without implying probability-based importance rankings.

7. Discussion and Selected Comparisons

7.1. Engineering Significance

The Jianzha case demonstrates that the realized performance of a safety-critical connection depends on the complete chain of design, manufacture, fabrication, installation, and acceptance rather than nominal fastener grade alone. Before arch closure, the distribution beam splice performed the function of a primary construction-stage member because it maintained a temporary support path for the incomplete cantilever. Its temporary designation and limited physical dimensions therefore did not reflect the consequences of its loss.

The case also illustrates the distinction between component resistance and system robustness. The official investigation identified a localized splice failure, while the present analysis interprets the visible sequence as showing that no effective arrest response became evident before secondary failures occurred. Whether residual support existed briefly, how much force it carried, and whether continuity was initially lost unilaterally or bilaterally remain unresolved. The engineering implication is that safety-critical temporary connections should be assessed both for their own limit states and for the system consequences of their removal.

7.2. Selection Basis and Comparison Framework

The six cases were purposively selected using the mechanism-based criteria in Section 2.5, and Table 8 summarizes their bounded, illustrative relevance to Jianzha without implying direct structural equivalence or independent validation of the Jianzha collapse mechanism.

Table 8. Illustrative mechanism-based comparison of Jianzha with selected historical bridge failures.

Case and Source	Construction or Loading State	Reported Initiating Deficiency and Propagation	Bounded Relevance to Jianzha
Quebec Bridge, Canada, 1907 [36]	Long-span steel cantilever truss under construction.	Deficient lower compression chord design failed under erection-stage stresses, followed by extensive collapse.	Local inadequacy in a primary erection-stage load path became critical under expected construction demand.
Second Narrows Bridge, Canada, 1958 [37,40]	Steel cantilever bridge supported by temporary erection works.	Inadequate design and checking of a temporary false bent initiated failure and collapse of the incomplete spans.	A temporary component governed the stability of a much larger incomplete structure.
Cleddau Bridge, United Kingdom, 1970 [38]	Steel box-girder bridge under cantilever erection.	Inadequate pier support diaphragm resistance under construction-stage compression led to collapse of the cantilevered system.	A localized force-transfer component was inadequate for the temporary erection state.
West Gate Bridge, Australia, 1970 [42,43]	Long-span steel box-girder bridge under construction.	Geometric incompatibility and corrective bolt removal at a critical splice preceded local instability and collapse.	Field response to fabrication/fit-up incompatibility affected a safety-critical connection region.
I-35W Bridge, United States, 2007 [19]	In-service steel deck truss bridge under concentrated reconstruction loads.	Undersized gusset plates lacked resistance under combined existing and construction loads; local connection failure propagated through the truss.	Actual connection resistance was lower than assumed, and construction-related demand activated the deficiency.
Chirajara Bridge, Colombia, 2018 [39]	Cable-stayed bridge approaching completion.	Inadequate tower diaphragm and transverse tie resistance caused tower failure and loss of the supported superstructure.	A localized load-transfer region failed while the incomplete structure depended strongly on the tower-and-cable system.

Note: Cases were purposively selected using the predefined criteria in Section 2.5 for illustrative mechanism-based comparison. The sample is not systematic, exhaustive, or statistically representative, and similarity to Jianzha is limited to the mechanism-level attributes stated in the final column.

7.3. Recurring Failure Pattern

Table 8 shows that the selected cases share a bounded mechanism rather than a common structural configuration. In each case, a localized deficiency occupied a consequential construction-stage or construction-related load path: a compression chord at Quebec [36],

temporary falsework at Second Narrows [37,40], a pier support diaphragm at Cleddau [38], an altered flange splice at West Gate [42,43], a gusset plate at I-35W [19], a tower diaphragm and transverse tie system at Chirajara [39], and a tower-top distribution beam splice at Jianzha [35]. Once the relevant demand was applied or the connection was altered, the surrounding structure could not redistribute or arrest the released actions before further failures developed. The comparison is limited to this mechanism-level similarity; it does not establish equivalence among the detailed causes, structural systems, or responsibilities associated with the individual accidents. For Jianzha, the comparison uses the officially identified bolt-group shear failure and splice separation as the initiating physical event and the author-derived load-path and barrier analyses developed in Sections 5 and 6.

7.4. Distinguishing Features and Comparative Synthesis

Jianzha differs materially from each comparator. The initiating deficiency was not established as an error in the permanent bridge concept (Quebec and Cleddau), a conventional ground-supported falsework failure (Second Narrows [37,40]), deliberate bolt removal from a loaded splice (West Gate), a defect activated after the bridge entered service (I-35W), or intrinsic failure of the principal tower system (Chirajara). The official investigation instead located the initiating weakness in the bolted splice of a temporary tower-top distribution beam and documented interacting deficiencies in material conformity, fabrication, installation, inspection, and governance [35]. These differences preclude direct causal equivalence.

An additional official construction-stage reference point is the 2018 Florida International University pedestrian bridge collapse. The NTSB identified errors in the design calculations, inadequate independent peer review of the individual construction stages and critical nodal region, and failure to close the roadway despite unresolved structural distress [27]. The case is retained as a contextual reference rather than as a principal comparator because its relevance to the present study concerns stage-specific design verification, response to observed distress, and personnel exposure more directly than the localized temporary load path and subsequent propagation mechanisms emphasized in the Table 8 comparison. It is therefore used to support the general recommendations on stage-specific checking, local detail verification, stop-work authority, and exclusion of exposed persons.

Overall, the comparison provides mechanism-level context but does not independently verify the Jianzha load-path or robustness interpretation; transferable implications are consolidated in Section 8.

8. Recommendations

Section 8 distinguishes accident-specific measures, established practices, and study-specific procedural refinements. The latter operationalize the barrier pathways identified in Section 6.5 through safety-critical component classification, complete local-detail verification, field-deviation hold points, formal load-transfer release, monitoring thresholds, robustness checks, assigned authority, and personnel exclusion. Implementation and verification requirements are specified below, with monitoring treated as supplementary to preventive controls.

8.1. Temporary Works Classification and Independent Verification

Temporary components should be classified according to their structural role and failure consequence, while the target reliability for a temporary construction stage should also account for its limited exposure duration. A temporary tower, cable, anchorage beam, distribution beam, splice, support, or backstay should be designated safety-critical where its loss could destabilize a substantial part of the incomplete bridge. Shorter exposure may

justify a lower target reliability than that adopted for permanent design situations where supported by the applicable reliability framework; however, the selected reliability level should remain commensurate with the consequences of failure, personnel exposure, and the criticality of the supported structure. Accordingly, design, fabrication, testing, inspection, acceptance, and monitoring requirements should be proportionate to the construction-stage risk rather than automatically equated with those for primary permanent members. The consequence-based reliability principle itself is established practice. The accident-specific procedural refinement proposed here is that the project should maintain an explicit register of safety-critical temporary components and connections, identified by the consequence of their loss, with the required level of analysis, checking, inspection, and release defined before those components enter service.

Construction-stage verification should represent the actual sequence, member activation, temporary loads, erection equipment, geometric nonlinearity, connection flexibility, asymmetric conditions, and credible component-loss scenarios. Independent checking should include local force-transfer zones, bolt groups, splice plates, diaphragms, anchorage assemblies, temporary bearings, and foundations rather than being limited to the global model.

8.2. Connection Quality, Fit-Up, and Hold Points

Safety-critical bolted connections should be verified as complete joint systems, including fastener material properties, thread position, hole geometry, plate contact, pretension where applicable, bearing, slip, eccentricity, and sequential engagement. Quality control should include batch-level traceability, independent mechanical testing, dimensional inspection, confirmation of installed bolt number and position, and inspection of safety-critical welds.

Material traceability, connection verification, and dimensional inspection are established quality control principles. The Jianzha-specific refinement proposed here is to convert any unresolved fit-up deviation in a safety-critical connection into a mandatory engineering hold point rather than permitting field accommodation without documented reassessment.

Fit-up problems—including hole mismatch, abnormal gaps, unexpected deformation, or inability to install specified fasteners—should trigger suspension, stabilization, as-built surveying, updated analysis, and written approval of an engineered corrective procedure. Uncontrolled hole enlargement, bolt omission, forced assembly, and improvised welding should be prohibited. Mandatory hold points should be established before use of temporary towers and critical splices, before major tensioning stages, during load transfer, and before closure.

8.3. Monitoring, Load Transfer, and Personnel Safety

Monitoring should supplement rather than replace procurement, testing, fabrication inspection, and formal acceptance. Global quantities such as cable force, cantilever geometry, and tower inclination should be combined, where practicable, with local strain, splice opening or slip, and connection-zone response. Stage-specific models should establish expected ranges and alert, action, and stop-work thresholds before loading begins.

Construction-stage monitoring and response verification are supported by established monitoring practice and literature. The specific refinement proposed here is the use of a formal hold-and-transfer gate after critical tensioning, so that operational completion is not defined solely by cessation of jacking or attainment of geometry but by documented confirmation of force transfer and response stability.

Critical tensioning should proceed incrementally, with verified structural response before each subsequent load step. Completion should include a documented hold-and-

transfer stage covering cessation of pumping, pressure holding, unloading, lock-off, transferred cable force, and response stability. Personnel should remain outside defined zones for collapse, falling objects, and cable recoils until transfer and stabilization are confirmed. Remote operation and automatic alarms or pump interlocks should be considered where communication and response delays could prevent timely intervention.

8.4. Robustness and Responsibility

Component-removal assessment should examine loss of cables, backstays, distribution beam splices, bolt rows, anchorage groups, temporary supports, and bracing. Where practical redundancy cannot be provided, passive arrest measures, enhanced verification, monitoring, and personnel exclusion should be required. Consequence-limiting measures should not depend on manual intervention after visible movement begins.

Component-removal and robustness assessments are established structural safety concepts. The accident-specific extension proposed here is to apply them explicitly to safety-critical temporary support paths and to link the resulting loss scenarios to both structural arrest provisions and personnel exposure controls before the relevant construction stage is authorized.

A project-specific responsibility matrix should assign authority for temporary system design, independent checking, supplier qualification, material testing, fabrication approval, field modifications, inspection, monitoring review, hold point release, tensioning authorization, and stop-work decisions. Safety-critical verification should not depend on informal assumptions that another organization has completed the required control.

Implementation should be verified through auditable project records rather than through general statements of compliance. For safety-critical temporary works, the minimum evidence should include a component criticality register; signed independent check records covering both global and local details; material certificates and batch mechanical test results; as-built dimensional and fastener installation records; documented engineering dispositions for field deviations; signed hold point and load-transfer release records; monitoring thresholds and response logs; component-removal or equivalent robustness assessments; personnel exclusion and remote operation plans where applicable; and a responsibility matrix identifying the individuals authorized to approve, release, suspend, or restart critical operations. Progression to the next safety-critical construction stage should require documented closure of the applicable controls.

9. Conclusions

This document-based study treats the official investigation as the controlling source for accident-specific findings; those findings are not claimed as original. Load-path tracing and conventional bolted connection mechanics are likewise not presented as novel methods. The contribution lies in the evidence-graded integration of the reported evidence with author-derived quantitative checks, load-path and topology interpretation, chronology, bounded robustness assessment, and safety barrier synthesis to derive transferable temporary works lessons.

The official investigation identified bolt-group shear failure and separation at the tower-top distribution beam splice as the initiating physical event. The bolt-level normalization developed here shows only that the reported material strength deficiency and threaded shear plane act cumulatively to reduce individual-fastener resistance; it does not quantify bolt-group or complete splice capacity. Before arch closure, the splice occupied a primary temporary support path. Visible cantilever descent preceded cable rupture by approximately 2 s, arch-rib fracture occurred at approximately +5 s, and extensive collapse developed by approximately +10 s. The nominal 5 min 40 s pre-movement interval is only

a temporal bound; the onset of splice damage and whether continuity loss was initially unilateral or bilateral remain unresolved.

The fault-tree and bow-tie synthesis organizes the reported technical and organizational deficiencies as failed preventive or detective controls and distinguishes alternative support and personnel exclusion as consequence-limiting controls. It identifies where the documented pathway could have been interrupted without assigning probabilities or quantitative importance. The historical comparison supports only a bounded mechanism-level conclusion: localized weakness in a consequential construction-stage load path can produce disproportionate collapse where redistribution or arrest capacity is insufficient.

The principal engineering implication is that temporary components should be governed by their structural role and failure consequence, while construction-stage reliability should also reflect exposure duration and project-specific risk. Safety-critical temporary works require stage-specific global and local verification, traceable materials, controlled fabrication and fit-up, formal hold points, supplementary monitoring, robustness assessment, clear responsibility, and personnel exclusion. Complete validation of the accident mechanism would require access to the original model, drawings, monitoring and test data, footage, and recovered components.

Funding: This research received no external funding.

Data Availability Statement: No new data were created or analyzed in this study.

Acknowledgments: During the preparation of this work, the author used ChatGPT (GPT-5.6 Sol) by OpenAI only for language refinement, readability improvement, and editorial polishing. After using this tool, the author reviewed and edited the content as needed and takes full responsibility for the content of the publication.

Conflicts of Interest: The author declares no conflicts of interest.

References

1. Sexsmith, R.G. Reliability during temporary erection phases. *Eng. Struct.* **1998**, *20*, 999–1003. [CrossRef]
2. Wang, P.-H.; Tang, T.-Y.; Zheng, H.-N. Analysis of cable-stayed bridges during construction by cantilever methods. *Comput. Struct.* **2004**, *82*, 329–346. [CrossRef]
3. Lozano-Galant, J.A.; Payá-Zaforteza, I.; Xu, D.; Turmo, J. Analysis of the construction process of cable-stayed bridges built on temporary supports. *Eng. Struct.* **2012**, *40*, 95–106. [CrossRef]
4. Zucca, M.; Tattoni, S.; Di Castri, M.; Simoncelli, M. On the collapse of a post-tensioned reinforced concrete truss bridge during the construction phases. *Eng. Fail. Anal.* **2024**, *158*, 107999. [CrossRef]
5. Wang, M.R.; Zhou, Z.J. Progressive collapse and structural robustness of bridges. *Appl. Mech. Mater.* **2012**, *193*, 1021–1024. [CrossRef]
6. Ghosn, M.; Moses, F.; Frangopol, D.M. Redundancy and robustness of highway bridge superstructures and substructures. *Struct. Infrastruct. Eng.* **2009**, *6*, 257–278. [CrossRef]
7. Tanner, P.; Hingorani, R.; Bellod, J.L.; Sanz, D. Thoughts on construction risk mitigation and acceptance. *Struct. Eng. Int.* **2018**, *28*, 60–70. [CrossRef]
8. André, J.; Beale, R.G.; Baptista, A.M. Recent advances and existing challenges in the design of bridge falsework systems. *Civ. Eng. Environ. Syst.* **2013**, *30*, 130–145. [CrossRef]
9. Prakhya, G.K.V. Temporary works in construction of bridges near third party assets. In *Structural Integrity and Failure*; IntechOpen: London, UK, 2021.
10. Duntemann, J.F.; Subrizi, C.D. Lessons learned from bridge construction failures. In *Forensic Engineering*; CRC Press: Boca Raton, FL, USA, 2000; pp. 374–385.
11. Hadipriono, F.C.; Wang, H.-K. Analysis of causes of falsework failures in concrete structures. *J. Constr. Eng. Manag.* **1986**, *112*, 112–121. [CrossRef]
12. Poon, S.; Price, A. Falsework and bridge failures. *Asia Pac. Build. Constr. Manag. J.* **1996**, *2*, 20–24.
13. Reddy, P.; Ghaboussi, J.; Hawkins, N.M. Simulation of construction of cable-stayed bridges. *J. Bridge Eng.* **1999**, *4*, 249–257. [CrossRef]

14. Pipinato, A.; Pellegrino, C.; Modena, C. Structural analysis of the cantilever construction process in cable-stayed bridges. *Period. Polytech. Civ. Eng.* **2012**, *56*, 1–26. Available online: https://hdl.handle.net/11577/2529652 (accessed on 1 June 2026). [CrossRef]
15. Sun, J.; Li, J.; Jiang, Y.; Ma, X.; Tan, Z.; Zhufu, G. Key construction technology and monitoring of long-span steel box tied arch bridge. *Int. J. Steel Struct.* **2023**, *23*, 191–207. [CrossRef]
16. Liu, D.; Tian, W.; Zheng, J. Long-span Steel Truss Arch Bridge Construction and Innovation. In Proceedings of the IABSE Conference: Structural Engineering: Providing Solutions to Global Challenges, Geneva, Switzerland, 23–25 September 2015; pp. 2086–2092.
17. Granata, M.F.; Margiotta, P.; Recupero, A.; Arici, M. Partial elastic scheme method in cantilever construction of concrete arch bridges. *J. Bridge Eng.* **2013**, *18*, 663–672. [CrossRef]
18. *BS 5975-1: 2024*; Temporary Works—Management Procedures for the Control of Temporary Works. Code of Practice. BSI: London, UK, 2024.
19. National Transportation Safety Board. *Collapse of I-35W Highway Bridge, Minneapolis, Minnesota, August 1, 2007*; Highway Accident Report NTSB/HAR-08/03; National Transportation Safety Board: Washington, DC, USA, 2008.
20. Reynolds, M.; Redl, E.; Uang, C.-M. Effect of bolt-hole clearance on the ultimate strength of eccentrically loaded bolt groups. *J. Struct. Eng.* **2021**, *147*, 04020285. [CrossRef]
21. RCSC. *Specification for Structural Joints Using High-Strength Bolts*; RCSC: Chicago, IL, USA, 2020.
22. Crawford, S.F.; Kulak, G.L. Eccentrically loaded bolted connections. *J. Struct. Div.* **1971**, *97*, 765–783. [CrossRef]
23. Caredda, G.; Porcu, M.C.; Buitrago, M.; Bertolesi, E.; Adam, J.M. Analysing local failure scenarios to assess the robustness of steel truss-type bridges. *Eng. Struct.* **2022**, *262*, 114341. [CrossRef]
24. Chen, Y.; Liao, Y.; Zhu, L.; Chen, L.; Chen, Y. Robustness of a Steel Truss Bridge Subjected to Sudden Member Breakage during the Continuous-to-Simply-Supported Transition. *Buildings* **2024**, *14*, 3035. [CrossRef]
25. Porcu, M.C.; Buitrago, M.; Calderón, P.A.; Garau, M.; Cocco, M.F.; Adam, J.M. Robustness-based assessment and monitoring of steel truss railway bridges to prevent progressive collapse. *J. Constr. Steel Res.* **2025**, *226*, 109200. [CrossRef]
26. Gaute-Alonso, A.; Garcia-Sanchez, D.; Alonso-Cobo, C.; Calderon-Uriszar-Aldaca, I. Temporary cable force monitoring techniques during bridge construction-phase: The Tajo River Viaduct experience. *Sci. Rep.* **2022**, *12*, 7689. [CrossRef] [PubMed]
27. National Transportation Safety Board. *Pedestrian Bridge Collapse Over SW 8th Street, Miami, Florida, March 15, 2018*; National Transportation Safety Board: Washington, DC, USA, 2019.
28. The Committee on Forensic Investigation of the Forensic Engineering Division of ASCE. *Guidelines for Failure Investigation*, 2nd ed.; Barrow, R.S., Anthony, R.W., Beasley, K.J., Verhulst, S.M., Eds.; ASCE: Reston, VA, USA, 2018.
29. de Ruijter, A.; Guldenmund, F. The bowtie method: A review. *Saf. Sci.* **2016**, *88*, 211–218. [CrossRef]
30. Sklet, S. Safety barriers: Definition, classification, and performance. *J. Loss Prev. Process Ind.* **2006**, *19*, 494–506. [CrossRef]
31. Reason, J. *Managing the Risks of Organizational Accidents*; Routledge: London, UK, 1997.
32. *IEC 31010:2019*; Risk Management—Risk Assessment Techniques, 2nd ed. IEC: Geneva, Switzerland, 2019.
33. Yan, Y. Design Research on a Long-Span Railway Continuous Steel Truss Arch Bridge. *Railw. Eng.* **2023**, *63*, 62–66. (In Chinese) [CrossRef]
34. Zhao, F. Key Design Technologies of Jianzha Yellow River Super Major Bridge on Xining-Chengdu Railway. *Railw. Stand. Des.* **2026**, *70*, 100–105. [CrossRef]
35. Team QPGAI, Ministry of Emergency Management of the People's Republic of China. *Investigation Report on the "8·22" Major Collapse Accident at the Jianzha Yellow River Super Bridge Construction Project of the Xining–Chengdu Railway*; Ministry of Emergency Management of the People's Republic of China: Beijing, China, 2026. (In Chinese)
36. Holgate, H.; Kerry, J.G.G.; Galbraith, J. *Royal Commission Quebec Bridge Inquiry Report*; Sessional Paper No. 154; SE Dawson: Ottawa, ON, Canada, 1908; Volumes I and II.
37. Betuzzi, L. Collapse of the Second Narrows Bridge during Construction. In Proceedings of the Congress on Technical Advancement 2017, Duluth, MN, USA, 10–13 September 2017; pp. 151–163.
38. HM Stationery Office. *Enquiry into the Basis of Design and Methods of Erection of Steel Box Girder Bridges*; Final Report of Committee, 4 Vols. (Commonly Known as "The Merrison Report"); Report No.: 0115503064; HM Stationery Office (HMSO): London, UK, 1973–1974; ISBN 978-0-11-550279-8.
39. Murphy, T.P.; Galindez, N.Y.; Artmont, F.A.; Adams, A.R.; Lopez de Murphy, M. Collapse of the Chirajara Cable-Stayed Bridge in Colombia. *Transp. Res. Rec.* **2025**, *2679*, 104–121. [CrossRef]
40. British Columbia Royal Commission. *Report of the British Columbia Royal Commission Second Narrows Bridge Inquiry*; Queen's Printer: Victoria, BC, Canada, 1958; Volume I.
41. *TB 10091-2017*; Code for Design of Steel Structures of Railway Bridges. China Railway Publishing House: Beijing, China, 2017. (In Chinese)
42. Gregson, S.; Humphrys, E. The West Gate Bridge collapse: How disaster happens. In *The Regulation and Management of Workplace Health and Safety*; Routledge: Abingdon, UK, 2020; pp. 32–51.

43. Victoria. Royal Commission into the Failure of West Gate Bridge. In *Report of Royal Commission into the Failure of West Gate Bridge*; 1971 Q624.4/1A1, TQ028210; Govt. Printer: Melbourne, Australia, 1971.
44. *GB/T 3098.1-2010*; Mechanical Properties of Fasteners—Bolts, Screws and Studs. China SAo: Beijing, China, 2011. (In Chinese)
45. *GB 50017-2017*; Standard for Design of Steel Structures. China Architecture & Building Press: Beijing, China, 2017. (In Chinese)

Disclaimer/Publisher's Note: The statements, opinions and data contained in all publications are solely those of the individual author(s) and contributor(s) and not of MDPI and/or the editor(s). MDPI and/or the editor(s) disclaim responsibility for any injury to people or property resulting from any ideas, methods, instructions or products referred to in the content.